Competing but Coexisting: Sulfate- and Potassium-Induced Supramolecular Motifs in Squaramide-Based Receptor Complexes

by

Damian Jagleniec, Marcin Wilczek, Łukasz Dobrzycki, Tomasz Marmur, Kamil Marcisz, Jan Romański

Faculty of Chemistry, University of Warsaw, Pasteura 1, PL 02-093 Warsaw, Poland

*jarom@chem.uw.edu.pl

TABLE OF CONTENTS

GENERAL INFORMATION

Unless specifically indicated, all other chemicals and reagents used in this study were purchased from commercial sources and used as received. If necessary purification of products was performed using column chromatography on silica gel (Merck Kieselgel 60, 230-400 mesh) with mixtures of chloroform/methanol. Thin-layer chromatography (TLC) was performed on silica gel plates (Merck Kieselgel 60 F254).

All NMR spectra used for products characterization, except for titrations, were recorded on Bruker AVANCE III HD 500 MHz spectrometer equipped with cryoprobe CPP BBO, at 25ºC in CD_3CN, using a residual protonated solvent signal as internal standard.

The ^1H NMR titrations were performed on a Bruker AVANCE III HD 300 MHz spectrometer, at 25ºC in CD_3CN. In each case, a 500 µL of freshly prepared ca. 3 mM solution of receptor in CD_3CN was added to a 5mm NMR tube. In the case of ion pair titration receptor was firstly pretreated with one equivalent of KPF_6 (refers to receptor). Then small aliquots of solution of KPF_6 or TBA_2SO_4, containing receptor at constant concentration, were added and a spectrum was acquired after each addition. The resulting titration data were analyzed using BindFit (v0.5) package, available online at http://supramolecular.org.

High resolution mass spectra (HRMS) were measured on a Quattro LC Micromass unit using ESI technique.

Dynamic Light Scattering analyses were performed using a Malvern Zetasizer Nano ZS (Malvern Instruments Ltd, UK) at 25ºC and a 173° angle relative to the source. The hydrodynamic diameter distributions were obtained by volume using the software package of the apparatus. Each curve represents the average of 3 measurements (16 runs each). Prior to analysis, all solutions were filtered and degassed.

SYNTHESIS

Preparation of Compound S1. A flask equipped with a stirring bar containing a solution of benzo-15- crown-5 (3 g, 11.18 mmol) in 75 ml of chloroform was placed in an ice-water bath at 0 °C. Concentrated nitric acid (15 ml) and 10 ml of glacial acid were added dropwise while keeping the temperature under 0 °C. The ice-water bath was removed and stirring was continued for 24 hours at room temperature. The reaction mixture was diluted with chloroform (50 ml) and shaken twice with ice distilled water (100 ml). The organic phases were collected and dried over anhydrous Na_2SO_4. The solvent was then removed under reduced pressure to give a yellow oil which was mixed with diethyl ether and kept in a freezer for 1 hours. The light yellow solid was isolated by filtration, washed with diethyl ether and dried in vacuo, to give desire product (3.22 g, 10.29 mmol, yield 92 %).
HRMS (ESI): calcd for $C_{14}H_{19}NO_7Na$ $[M+Na]^+$: 336.1059, found: 336.1061.
^{1}H NMR (300 MHz, DMSO-d_6) δ 7.95 – 7.85 (1H, m), 7.77 – 7.70 (1H, m), 7.21 – 7.09 (1H, m), 4.25 – 4.13 (4H, m), 3.88 – 3.74 (4H, m), 3.68 – 3.58 (8H, m).
^{13}C NMR (75 MHz, DMSO-d_6) δ 154.9, 148.6, 141.1, 118.3, 112.3, 108.3, 71.0, 70.1, 70.0, 69.3, 69.2, 68.9, 69.8.
Preparation of Compound S2. A flask equipped with a stirring bar containing a solution of benzo-18- crown-6 (2 g, 6.4 mmol) in 50 ml of chloroform was placed in an ice-water bath at 0 °C. Concentrated nitric acid (10 ml) and 5 ml of glacial acid were added dropwise while keeping the temperature under 0 °C. The ice-water bath was removed and stirring was continued for 24 hours at room temperature. The reaction mixture was diluted with chloroform (30 ml) and shaken twice with ice distilled water (100 ml). The organic phases were collected and dried over anhydrous Na_2SO_4. The solvent was then removed under reduced pressure to give a yellow oil which was mixed with diethyl ether and kept in a freezer for 1 hours. The light yellow solid was isolated by filtration, washed with diethyl ether and dried in vacuo, to give desire product (2.19 g, 6.14 mmol, yield 96 %).
HRMS (ESI): calcd for $C_{16}H_{23}NO_8Na$ $[M+Na]^+$: 380.1322, found: 380.1331.
^{1}H NMR (300 MHz, DMSO-d_6) δ 7.93 – 7.85 (1H, m), 7.75 – 7.71 (1H, m), 7.22 – 7.13 (1H, m), 4.31 – 4.12 (4H, m), 3.85 – 3.72 (4H, m), 3.68 – 3.45 (12H, m).
^{13}C NMR (75 MHz, DMSO-d_6) δ 154.5, 148.3, 141.0, 118.1, 112.1, 107.6, 70.4, 70.3, 70.3, 70.1, 69.2, 69.0, 68.8, 68.7.
Preparation of receptor 1. To a degassed solution of 4-nitrobenzo-15-crown-5-ether **S1** (940 mg, 3 mmol) in 50 ml of THF/MeOH (1:4) 25 mg of 10% Pd/C was added. The reaction mixture was kept under H_2 atmosphere (balloon pressure) at room temperature overnight. The catalyst was removed by filtration through a pad of Celite and washed with MeOH. The filtrate was concentrated under reduced pressure to give the crude product **A1** in quantitative yield (856 mg). The amine was used in next step without further purification.
To the solution of amine **A1** (456 mg, 1.61 mmol) in MeOH (5 ml) was added compound **S3** (543 mg, 1.60 mmol) at rt. The mixture was stirred at room temperature for 2 days. The reaction mixture was filtrated and collected solid material was washed with MeOH. The obtained white solid was dried *in vacuo* to give desired receptor **1** (900 mg, 1.45 mmol, 90%).
HRMS (ESI): calcd for $C_{26}H_{24}F_6N_2O_7Na$ $[M + Na]^+$: 613.1385, found: 613.1379.
^{1}H NMR (300 MHz, DMSO-d_6) δ 10.22 (1H, s), 9.97 (1H, s), 8.15 – 7.95 (2H, m), 7.78 – 7.65 (1H, s), 7.31 – 7.11 (1H, m), 7.02 – 6.91 (1H, m), 6.90 – 6.81 (1H, m), 4.13 – 3.99 (4H, m), 3.85 – 3.71 (4H, m), 3.70 – 3.45 (8H, m).
^{13}C NMR (75 MHz, DMSO-d_6) δ 182.8, 181.3, 166.4, 163.8, 149.1, 145.3, 140.6, 131.8, 131.3, 130.9, 130.4, 124.6, 121.0, 118.2, 115.2, 114.7, 111.1, 106.2, 70.1, 70.0, 69.7, 69.5, 69.2, 68.7, 68.4, 68.4.
Preparation of receptor 2. To a degassed solution of 4-nitrobenzo-18-crown-6-ether **S2** (645 mg, 1.8 mmol) in 30 ml of THF/MeOH (1:4) 25 mg of 10% Pd/C was added. The reaction mixture was kept under H_2 atmosphere (balloon pressure) at room temperature overnight. The catalyst was removed by filtration through a pad of Celite and washed with MeOH. The filtrate was concentrated under reduced pressure to give the crude product **A2** in quantitative yield (602 mg). The amine **A2** was used in next step without further purification.
To the solution of amine **A2** (602 mg, 1.84 mmol) in MeOH (10 ml) was added a compound **S3** (680 mg, 2.0 mmol) at rt. The mixture was stirred at room temperature for 2 days in Ar atmosphere. The reaction mixture was

filtrated and collected solid material was washed with MeOH. Obtained white solid was dried *in vacuo* to give desired **2** in 90 % yield (1.05 g, 1.65 mmol).
HRMS (ESI): calcd for $C_{28}H_{28}F_6N_2O_8K$ $[M+K]^+$: 673.1387, found: 673.1375.
^{1}H NMR (300 MHz, DMSO-d_6) δ 10.20 (s, 1H), 9.96 (s, 1H), 8.09 – 8.01 (m, 2H), 7.78 – 7.69 (m, 1H), 7.24 – 7.17 (m, 1H), 6.98 – 6.90 (m, 1H), 6.86 – 6.77 (m, 1H), 4.15 – 4.00 (m, 4H), 3.82 – 3.70 (m, 4H), 3.68 – 3.46 (m, 12H).
^{13}C NMR (75 MHz, DMSO-d_6) δ 183.6, 181.9, 166.8, 164.4, 149.1, 145.3, 141.2, 132.4, 132.1, 131.9, 131.5, 125.4, 121.8, 119.0, 115.8, 114.2, 111.3, 105.7, 70.3, 70.3, 69.2, 69.0, 68.9, 68.5.
Preparation of compound S3. To a solution of 3,4-dimethoxy-3-cyclobutane-1,2-dione (1.5 g, 10.57 mmol) in MeOH (15 ml) was added 3,5-bis(trifluoromethyl)aniline (1.8 ml, 11.62 mmol) was added at room temperature. After being stirred for 3 days the reaction mixture was filtered, and the collected solid material was washed with MeOH. The obtained light yellow solid was dried *in vacuo* to give product **S3** (3.40 g, 10.04 mmol).
HRMS (ESI): calcd for $C_{13}H_7F_6NO_3Na$ $[M+Na]^+$: 362.0228, found: 362.0225.
^{1}H NMR (300 MHz, DMSO-d_6) δ 11.19 (s, 1H), 8.05 (m, 2H), 7.79 (m, 1H), 4.42 (s, 3H).
^{13}C NMR (75 MHz, DMSO-d_6) δ 187.4, 184.5, 179.9, 169.1, 139.9, 131.4 (q, J = 33 Hz), 131.0 (q, J = 271 Hz), 130.5, 124.9, 121.3, 119.2, 116.1, 60.9.
Preparation of receptor 3. To a solution of compound **S3** (300 mg, 0.88 mmol) in MeOH (20 ml) was added aniline (82 mg, 0.88 mmol) at room temperature. The mixture was stirred for 2 days. Then the reaction mixture was filtered, and the collected solid material was washed with MeOH. The obtained white solid was dried *in vacuo* to give the desired receptor **3** (260 mg, 0.65 mmol, 74 %).
HRMS (ESI): calcd for $C_{13}H_7F_6NO_3Na$ $[M+Na]^+$: 362.0228, found: 362.0225.
^{1}H NMR (300 MHz, CD_3CN-d_3) δ 8.41 – 8.19 (m, 2H), 8.04 – 7.92 (m, 2H), 7.71 – 7.61 (m, 1H), 7.48 – 7.32 (m, 4H), 7.21 – 7.12 (m, 1H).
^{13}C NMR (75 MHz, DMSO-d_6) δ 182.5, 181.9, 166.5, 140.5, 137.9, 131.8, 131.3 (q, J = 32 Hz), 130.9, 130.4, 128.9, 120.9, 118.6, 118.3, 114.8.

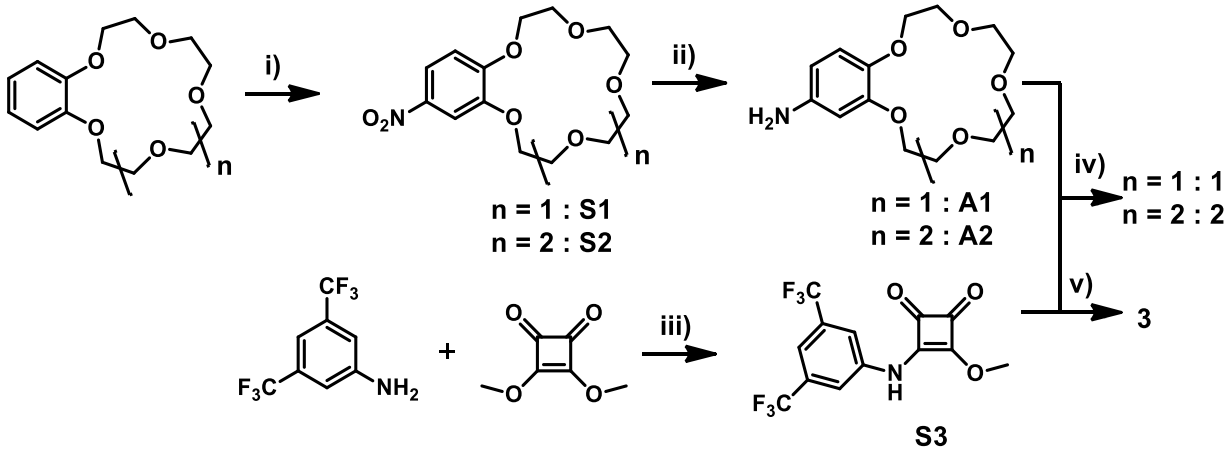

Scheme 1. Synthesis of receptors **1** – **3**. Reagents and conditions: i) chloroform, benzo-15-crown-5 or benzo-18-crown-6, HNO_3, CH_3COOH, 0 ºC, 92 % (**S1**) and 96 % (**S2**); ii) H_2, Pd/C, MeOH/THF, 12 h, r.t., quantitative; iii) 3,5-Bis(trifluoromethyl)aniline, methanol, 48 h, r.t., 95 %; iv) methanol, **S3**, 24 h, r.t., 90 % (**1**) and 90 % (**2**); v) methanol, aniline, 48 h, r.t., 74 %.

NMR MEASUREMENTS (TITRATIONS)

Figure S1. Partial ^{1}H NMR spectra and titrations curves recorded upon titration of receptor **1** in CD_3CN with KPF_6: a) and b) – aromatic proton signals, c) and d) – crown ether proton signals.

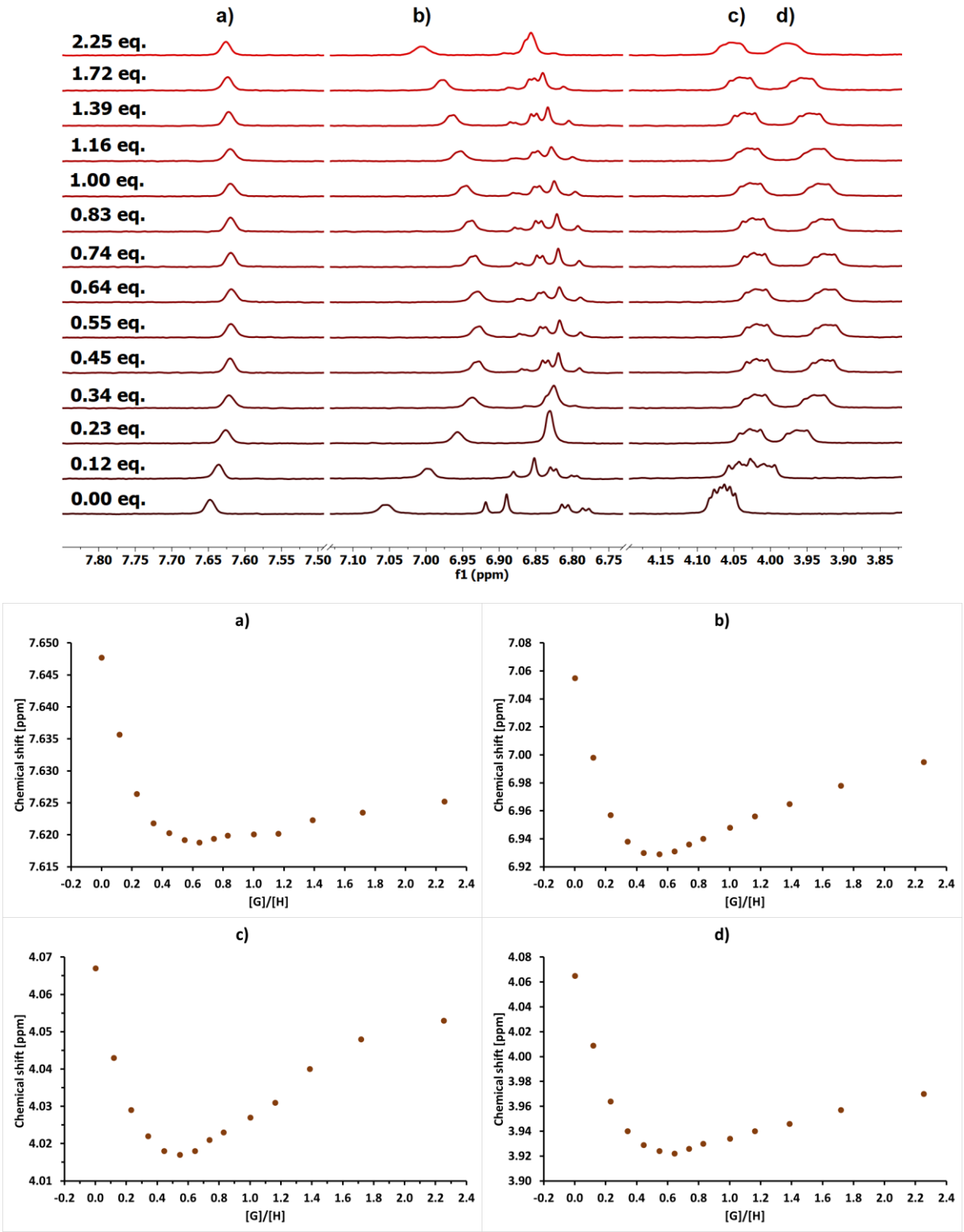

Figure S2. Partial ^{1}H NMR spectra and titrations curves recorded upon titration of receptor **1** in CD_3CN with TBA_2SO_4: a) and b) – aromatic protons signals, c) and d) – crown ether protons signals.

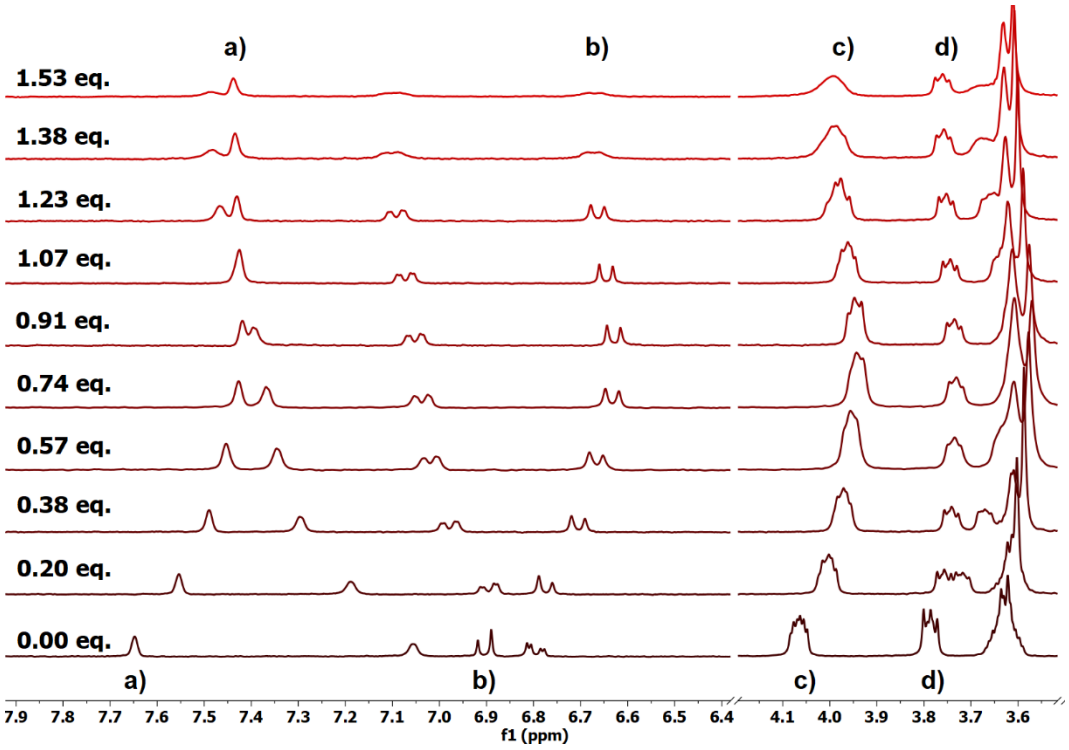

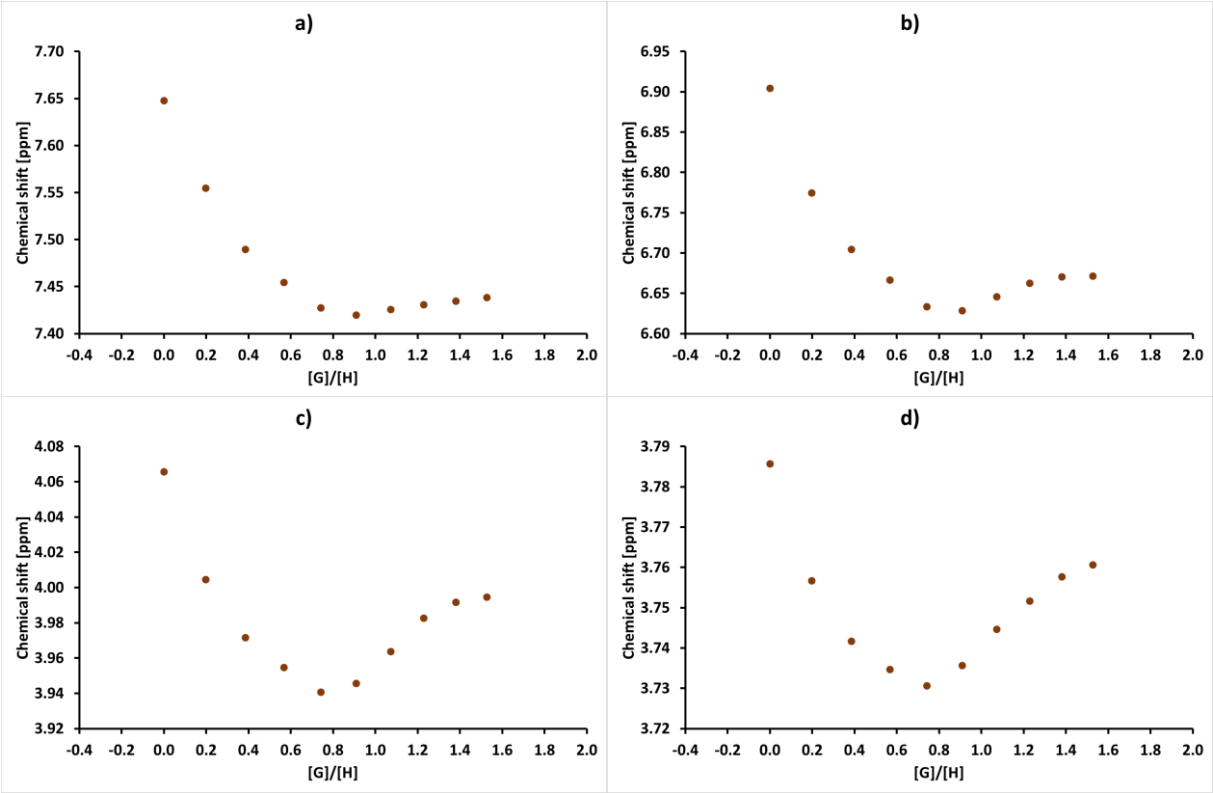

Figure S3. Partial ^{1}H NMR spectra and titrations curves recorded upon titration of receptor **1** in CD_3CN with TBA_2SO_4 in the presence of 1 equivalent of KPF_6: a), b) and c) – aromatic proton signals, d) – crown ether proton signals.

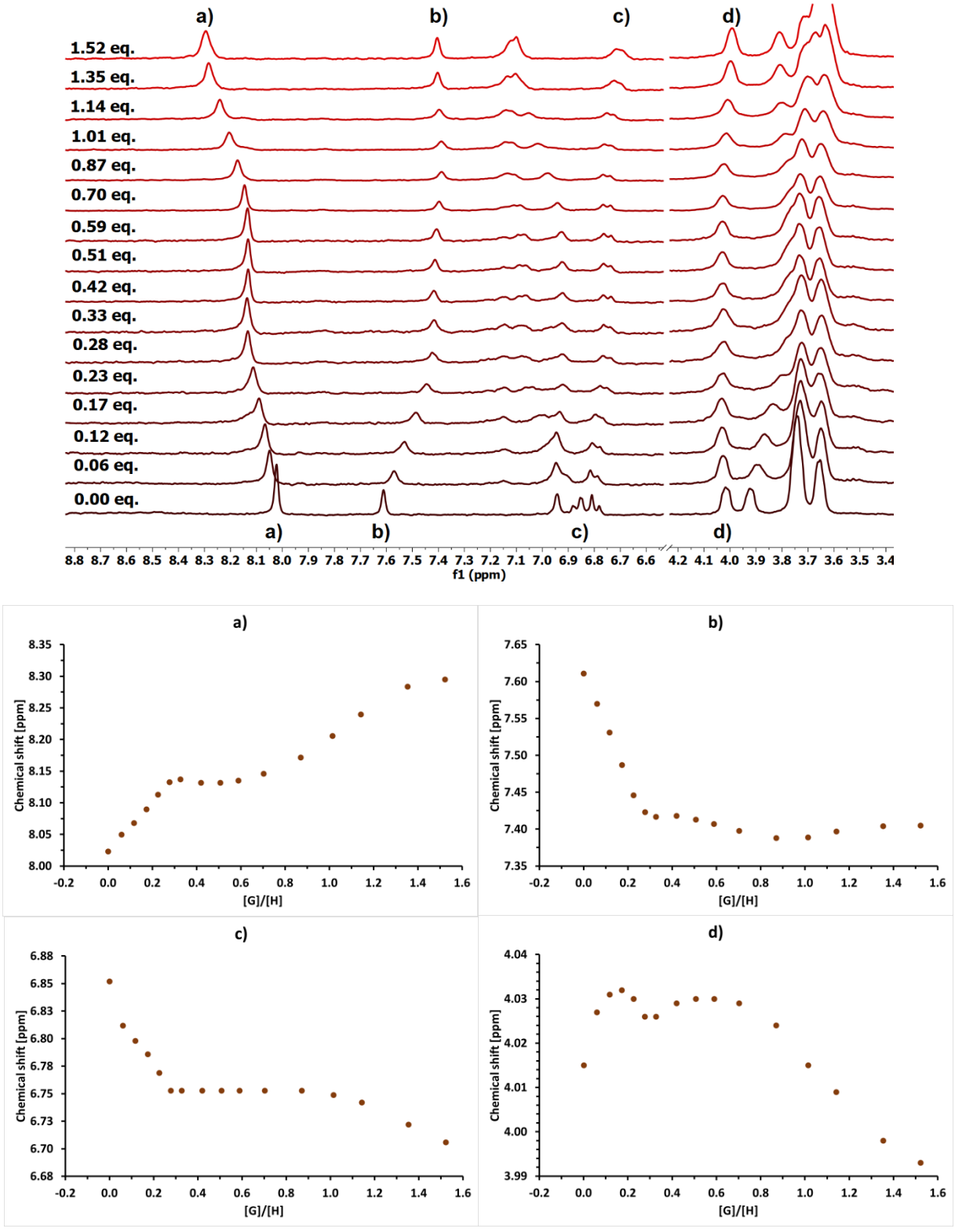

DIFFUSION ANALYSIS DATA

Analysis of the diffusion coefficient for receptor 1 was carried out by fitting the signal attenuation curves obtained from diffusion NMR experiments. In Figures S4–S19, the horizontal axis (X) denotes the gradient strength, and the vertical axis (Y) represents the NMR signal intensity.

Figure S4. Analysis of the diffusion coefficient for receptor **1**.

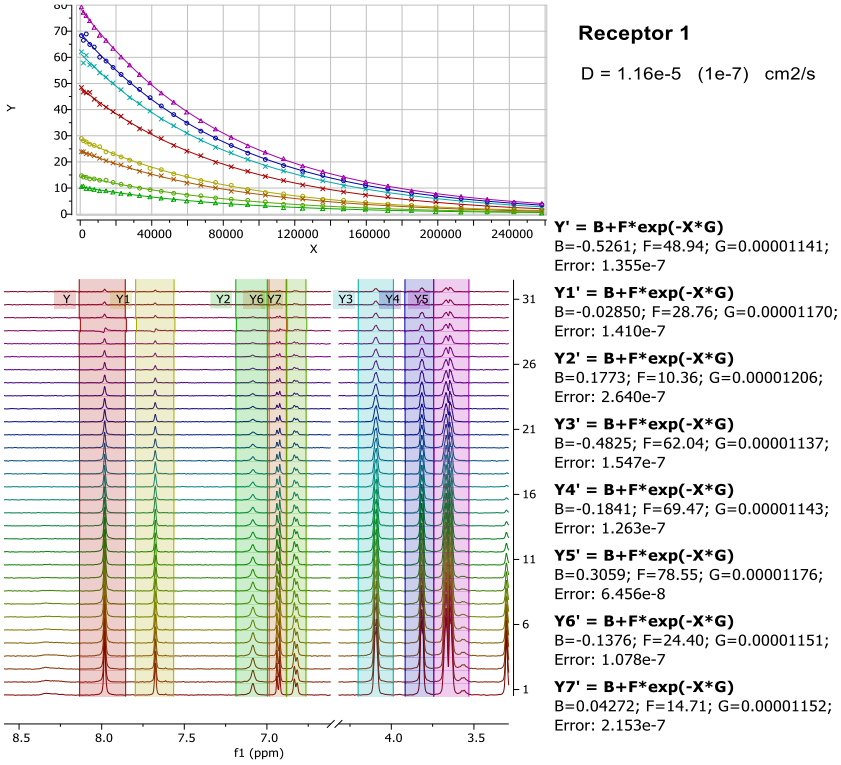

Figure S5. Analysis of the diffusion coefficient for receptor **1** with 1 eq. of KPF_6.

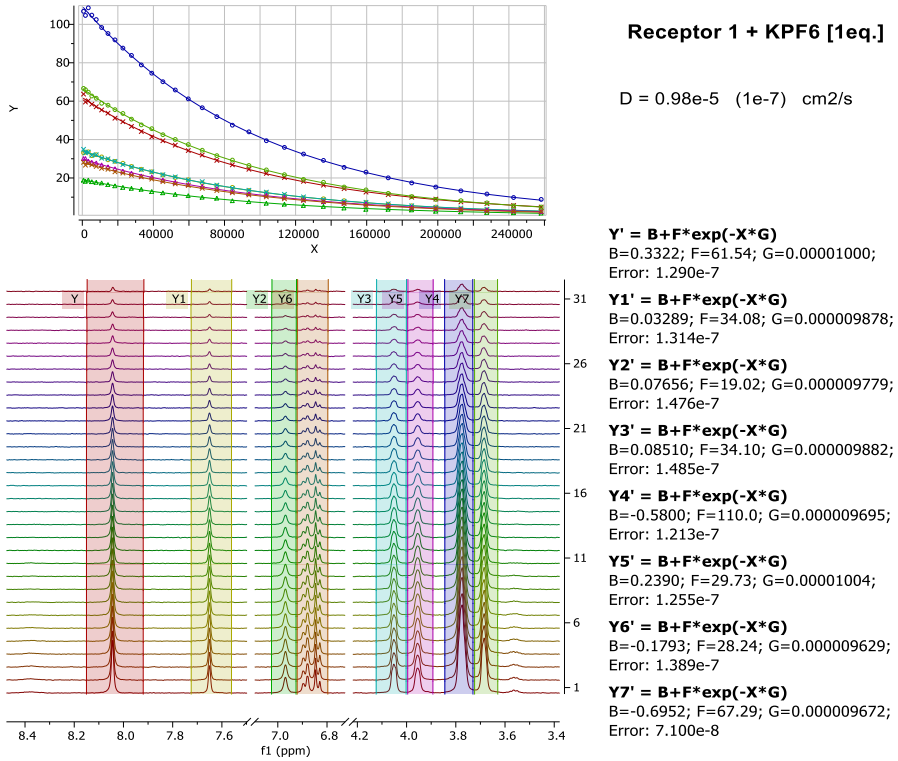

Figure S6. Analysis of the diffusion coefficient for receptor **1** with 0.25 eq. of TBA_2SO_4.

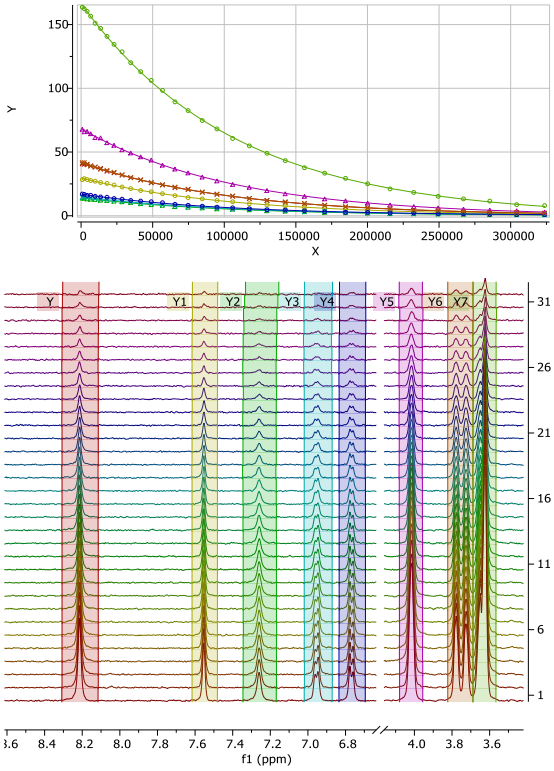

Receptor 1 + TBA2SO4 [0.25]

D = 0.96e-5 (1e-7) cm2/s

Y' = B+F*exp(-X*G)
B=-0.1143; F=41.76; G=0.000009474;
Error: 7.575e-8

Y1' = B+F*exp(-X*G)
B=-0.05278; F=29.61; G=0.000009469;
Error: 9.532e-8

Y2' = B+F*exp(-X*G)
B=0.05683; F=14.00; G=0.000009645;
Error: 1.301e-7

Y3' = B+F*exp(-X*G)
B=0.1937; F=14.80; G=0.000009790;
Error: 1.774e-7

Y4' = B+F*exp(-X*G)
B=0.1783; F=16.82; G=0.000009737;
Error: 1.322e-7

Y5' = B+F*exp(-X*G)
B=-0.3143; F=68.70; G=0.000009457;
Error: 7.306e-8

Y6' = B+F*exp(-X*G)
B=0.3044; F=41.76; G=0.000009734;
Error: 7.124e-8

Y7' = B+F*exp(-X*G)
B=-0.8345; F=167.3; G=0.000009330;
Error: 4.260e-8

Figure S7. Analysis of the diffusion coefficient for receptor **1** with 1 eq. of TBA_2SO_4.

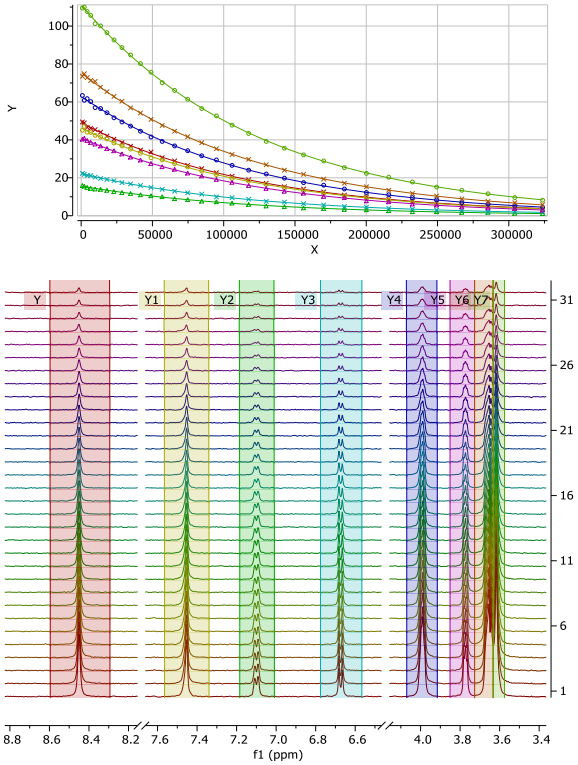

Receptor 1 + TBA2SO4 [1eq.]

D = 0.81e-5 (1e-7) cm2/s

Y' = B+F*exp(-X*G)
B=0.4056; F=48.65; G=0.000008227;
Error: 8.300e-8

Y1' = B+F*exp(-X*G)
B=0.1692; F=46.05; G=0.000008030;
Error: 1.134e-7

Y2' = B+F*exp(-X*G)
B=0.04508; F=15.56; G=0.000008224;
Error: 1.317e-7

Y3' = B+F*exp(-X*G)
B=0.2647; F=21.93; G=0.000008278;
Error: 1.039e-7

Y4' = B+F*exp(-X*G)
B=0.1148; F=62.78; G=0.000008185;
Error: 8.537e-8

Y5' = B+F*exp(-X*G)
B=-0.03271; F=41.03; G=0.000008020;
Error: 5.786e-8

Y6' = B+F*exp(-X*G)
B=0.03138; F=75.41; G=0.000007988;
Error: 6.132e-8

Y7' = B+F*exp(-X*G)
B=-0.1577; F=111.3; G=0.000007932;
Error: 4.947e-8

Figure S8. Analysis of the diffusion coefficient for receptor **1** with 1 eq. of KPF_6 and 0.25 eq. of TBA_2SO_4.

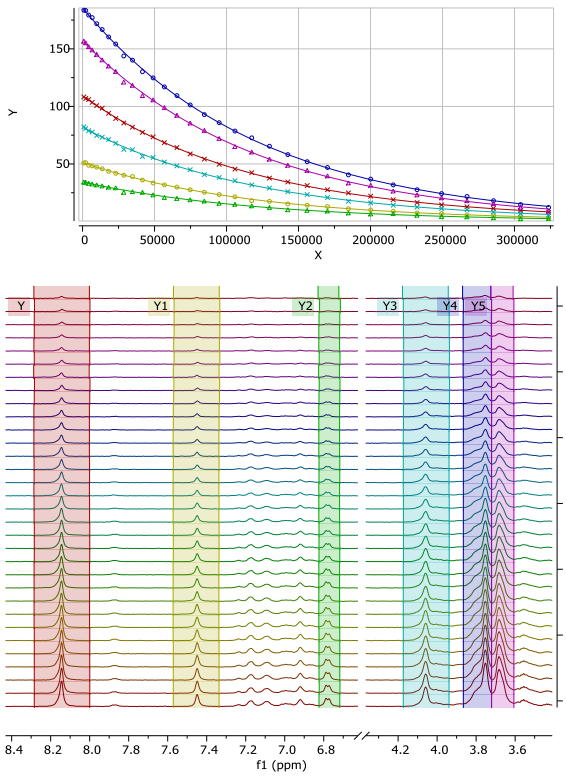

Receptor 1 + K [1eq.] +TBA2SO4 [0.25eq.]

D = 0.82e-5 (1e-7) cm2/s

Y' = B+F*exp(-X*G)
B=0.9837; F=108.2; G=0.000008291;
Error: 4.626e-8

Y1' = B+F*exp(-X*G)
B=0.4319; F=50.78; G=0.000008431;
Error: 9.957e-8

Y2' = B+F*exp(-X*G)
B=0.02252; F=34.39; G=0.000008111;
Error: 1.856e-7

Y3' = B+F*exp(-X*G)
B=0.3141; F=81.49; G=0.000008139;
Error: 1.074e-7

Y4' = B+F*exp(-X*G)
B=-0.4349; F=186.0; G=0.000008098;
Error: 6.277e-8

Y5' = B+F*exp(-X*G)
B=-0.3898; F=157.4; G=0.000008160;
Error: 7.552e-8

Figure S9. Analysis of the diffusion coefficient for the second component in the solution of receptor **1** with 1 eq. of KPF_6 and 0.25 eq. of TBA_2SO_4.

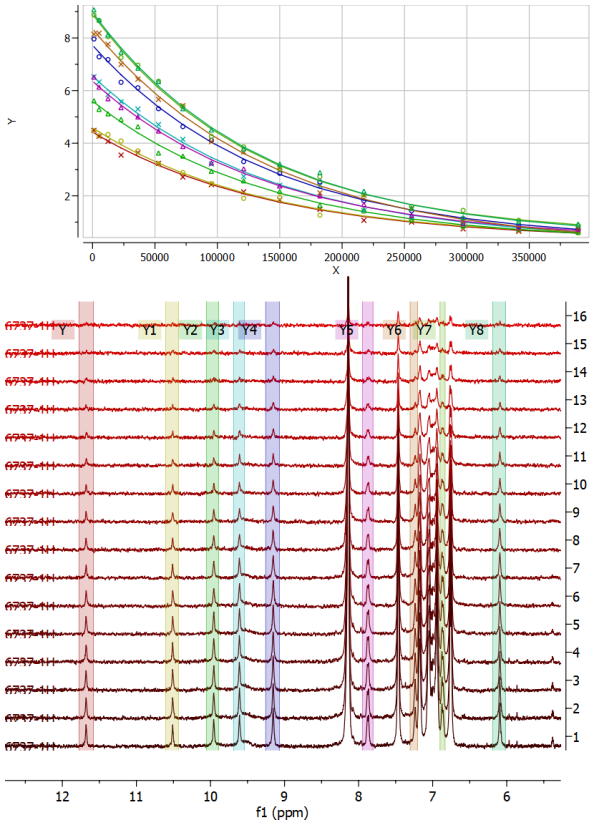

Receptor 1 + K [1eq.] + TBA2SO4 [0.25eq.] (second component)

D = 0.72e-5 (3e-7) cm2/s

Y' = B+F*exp(-X*G)
B=0.3064; F=4.118; G=0.000006964;
Error: 3.672e-7

Y1' = B+F*exp(-X*G)
B=0.3655; F=4.224; G=0.000007268;
Error: 4.218e-7

Y2' = B+F*exp(-X*G)
B=0.2324; F=5.368; G=0.000007034;
Error: 3.172e-7

Y3' = B+F*exp(-X*G)
B=0.2167; F=6.335; G=0.000007039;
Error: 3.690e-7

Y4' = B+F*exp(-X*G)
B=0.2646; F=7.461; G=0.000007164;
Error: 2.785e-7

Y5' = B+F*exp(-X*G)
B=0.3082; F=6.051; G=0.000007153;
Error: 2.332e-7

Y6' = B+F*exp(-X*G)
B=0.07783; F=8.267; G=0.000007023;
Error: 3.040e-7

Y7' = B+F*exp(-X*G)
B=0.4767; F=8.429; G=0.000007673;
Error: 2.577e-7

Y8' = B+F*exp(-X*G)
B=0.3972; F=8.575; G=0.000007502;
Error: 2.252e-7

Figure S10. Analysis of the diffusion coefficient for receptor **2**.

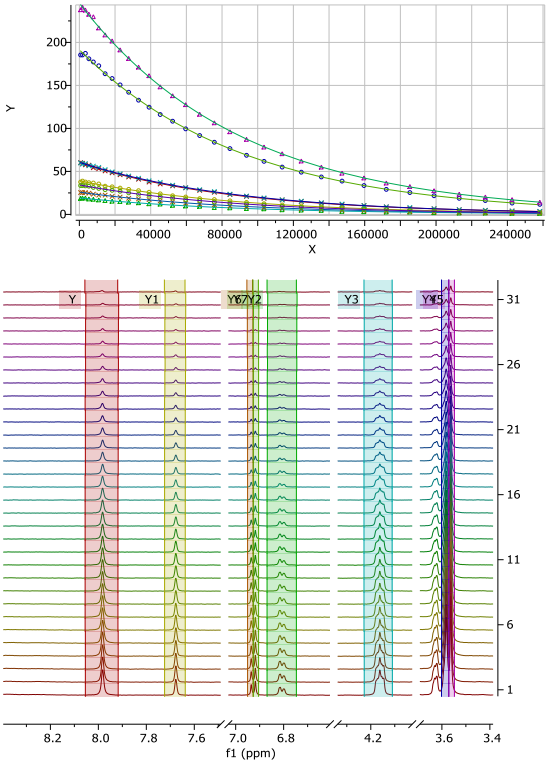

Receptor 2

D = 1.11e-5 (2e-7) cm2/s

Y' = B+F*exp(-X*G)
B=0.3105; F=59.70; G=0.00001142;
Error: 1.085e-7

Y1' = B+F*exp(-X*G)
B=-0.2656; F=39.32; G=0.00001079;
Error: 1.419e-7

Y2' = B+F*exp(-X*G)
B=0.1416; F=19.09; G=0.00001111;
Error: 1.616e-7

Y3' = B+F*exp(-X*G)
B=-0.2748; F=60.90; G=0.00001098;
Error: 9.806e-8

Y4' = B+F*exp(-X*G)
B=-0.4174; F=191.9; G=0.00001085;
Error: 1.030e-7

Y5' = B+F*exp(-X*G)
B=-0.1567; F=245.8; G=0.00001099;
Error: 9.278e-8

Y6' = B+F*exp(-X*G)
B=0.1061; F=25.80; G=0.00001114;
Error: 1.279e-7

Y7' = B+F*exp(-X*G)
B=0.05090; F=34.25; G=0.00001125;
Error: 8.677e-8

Figure S11. Analysis of the diffusion coefficient for receptor **2** with 1 eq. of KPF_6.

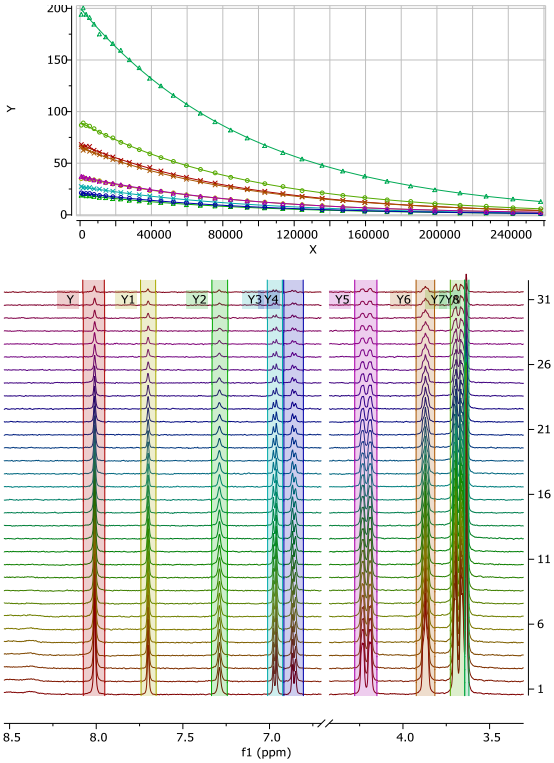

Receptor 2 + KPF6 [1 eq.]

D = 1,06e-5 (1e-7) cm2/s

Y' = B+F*exp(-X*G)
B=-0.4076; F=68.70; G=0.00001057;
Error: 1.123e-7

Y1' = B+F*exp(-X*G)
B=0.03412; F=36.22; G=0.00001053;
Error: 1.348e-7

Y2' = B+F*exp(-X*G)
B=0.2091; F=19.26; G=0.00001090;
Error: 1.942e-7

Y3' = B+F*exp(-X*G)
B=-0.1701; F=27.66; G=0.00001048;
Error: 1.305e-7

Y4' = B+F*exp(-X*G)
B=-0.1339; F=21.43; G=0.00001036;
Error: 1.540e-7

Y5' = B+F*exp(-X*G)
B=0.3464; F=36.96; G=0.00001095;
Error: 8.993e-8

Y6' = B+F*exp(-X*G)
B=0.2083; F=65.03; G=0.00001072;
Error: 9.821e-8

Y7' = B+F*exp(-X*G)
B=0.001677; F=89.79; G=0.00001059;
Error: 9.684e-8

Y8' = B+F*exp(-X*G)
B=-0.6708; F=201.2; G=0.00001046;
Error: 1.059e-7

Figure S12. Analysis of the diffusion coefficient for receptor **2** with 0.25 eq. of TBA_2SO_4.

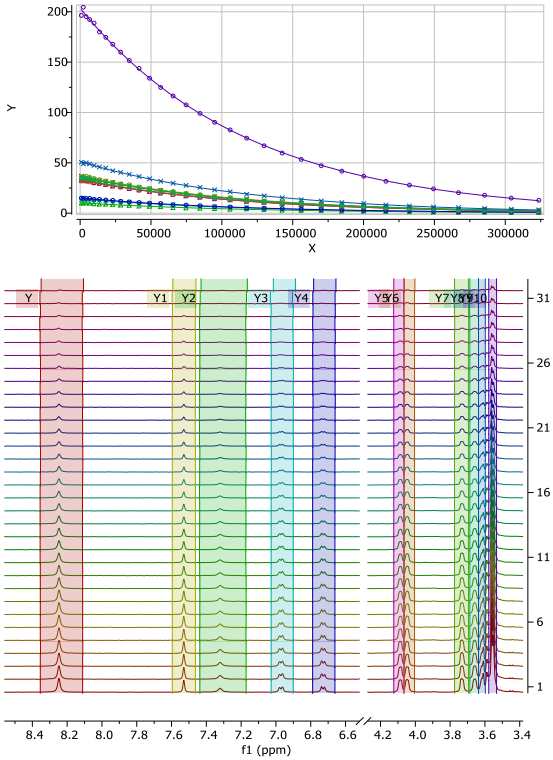

Y' = B+F*exp(-X*G)
B=-0.1257; F=36.65; G=0.000008548;
Error: 6.661e-8

Y1' = B+F*exp(-X*G)
B=-0.3124; F=32.86; G=0.000008344;
Error: 8.409e-8

Y2' = B+F*exp(-X*G)
B=0.1382; F=10.20; G=0.000008715;
Error: 1.876e-7

Y3' = B+F*exp(-X*G)
B=0.01993; F=14.20; G=0.000008583;
Error: 1.979e-7

Y4' = B+F*exp(-X*G)
B=0.008700; F=15.14; G=0.000008597;
Error: 1.426e-7

Y5' = B+F*exp(-X*G)
B=0.3250; F=33.15; G=0.000008972;
Error: 8.075e-8

Y6' = B+F*exp(-X*G)
B=0.01907; F=33.90; G=0.000008772;
Error: 6.633e-8

Y7' = B+F*exp(-X*G)
B=0.05651; F=37.17; G=0.000008485;
Error: 1.122e-7

Y8' = B+F*exp(-X*G)
B=0.2692; F=35.93; G=0.000008710;
Error: 9.109e-8

Y9' = B+F*exp(-X*G)
B=-0.3582; F=51.65; G=0.000008296;
Error: 8.474e-8

Y10' = B+F*exp(-X*G)
B=-0.6909; F=204.2; G=0.000008485;
Error: 8.868e-8

Receptor 2
+ TBA2SO4 [0.25eq.]

D = 0.86e-5 (1e-7) cm2/s

Figure S13. Analysis of the diffusion coefficient for receptor **2** with 1 eq. of TBA_2SO_4.

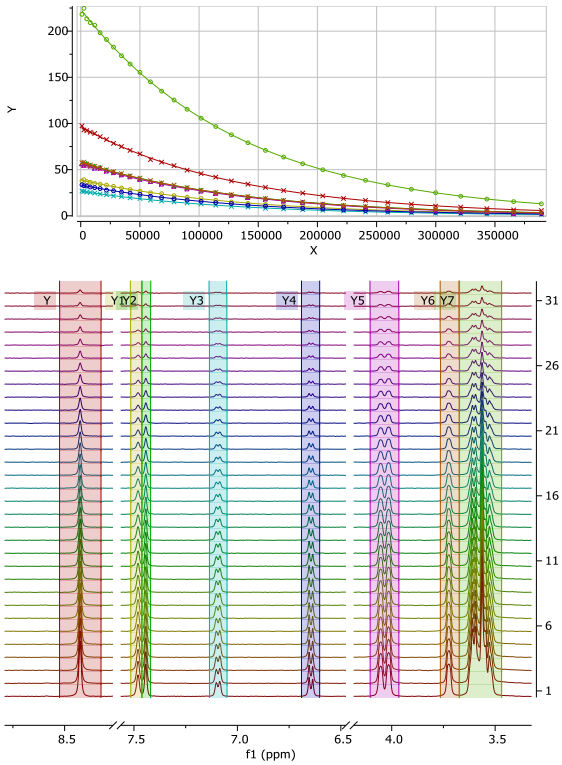

Receptor 2 + TBA2SO4 [1eq.]

D = 0.73e-5 (1e-7) cm2/s

Y' = B+F*exp(-X*G)
B=0.3053; F=96.15; G=0.000007393;
Error: 6.573e-8

Y1' = B+F*exp(-X*G)
B=0.1238; F=38.62; G=0.000007331;
Error: 7.987e-8

Y2' = B+F*exp(-X*G)
B=0.06944; F=58.15; G=0.000007285;
Error: 7.223e-8

Y3' = B+F*exp(-X*G)
B=-0.1499; F=26.92; G=0.000007329;
Error: 5.512e-8

Y4' = B+F*exp(-X*G)
B=0.3120; F=33.05; G=0.000007557;
Error: 5.646e-8

Y5' = B+F*exp(-X*G)
B=-0.5872; F=57.45; G=0.000007219;
Error: 6.971e-8

Y6' = B+F*exp(-X*G)
B=-0.1905; F=58.64; G=0.000007263;
Error: 4.576e-8

Y7' = B+F*exp(-X*G)
B=0.2821; F=223.3; G=0.000007358;
Error: 6.254e-8

Figure S14. Analysis of the diffusion coefficient for receptor **2** with 1 eq. of KPF_6 and 0.25 eq. of TBA_2SO_4.

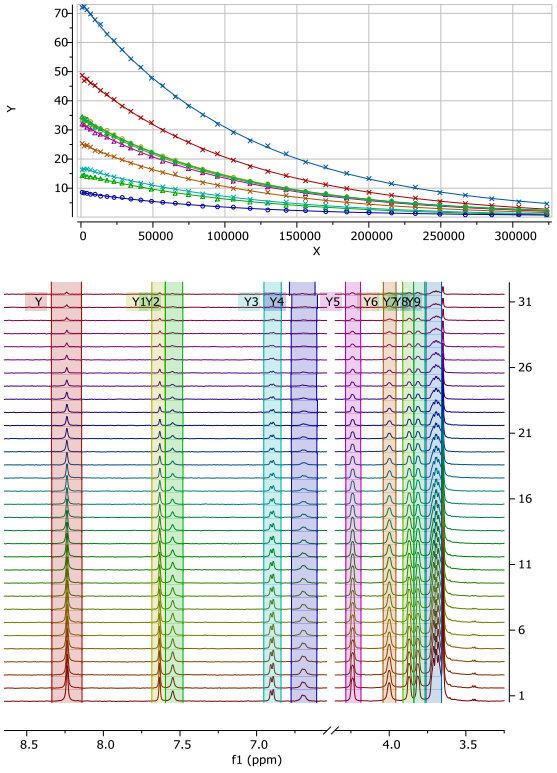

Receptor 2 + K [1eq.] + TBA2SO4 [0.25eq]

D = 0.89e-5 (3e-7) cm2/s

Y' = B+F*exp(-X*G)
B=-0.2823; F=49.23; G=0.000008557;
Error: 7.214e-8

Y1' = B+F*exp(-X*G)
B=-0.03298; F=34.45; G=0.000008621;
Error: 1.035e-7

Y2' = B+F*exp(-X*G)
B=-0.03986; F=14.84; G=0.000008531;
Error: 1.370e-7

Y3' = B+F*exp(-X*G)
B=0.1442; F=16.79; G=0.000008692;
Error: 1.699e-7

Y4' = B+F*exp(-X*G)
B=0.4356; F=8.115; G=0.000009684;
Error: 1.888e-7

Y5' = B+F*exp(-X*G)
B=0.3394; F=31.78; G=0.000008856;
Error: 7.472e-8

Y6' = B+F*exp(-X*G)
B=0.1995; F=25.11; G=0.000008825;
Error: 1.062e-7

Y7' = B+F*exp(-X*G)
B=0.6227; F=33.15; G=0.000009098;
Error: 1.161e-7

Y8' = B+F*exp(-X*G)
B=0.5762; F=33.84; G=0.000009005;
Error: 8.772e-8

Y9' = B+F*exp(-X*G)
B=0.4670; F=73.23; G=0.000008767;
Error: 6.353e-8

Figure S15. Analysis of the diffusion coefficient for receptor **3**.

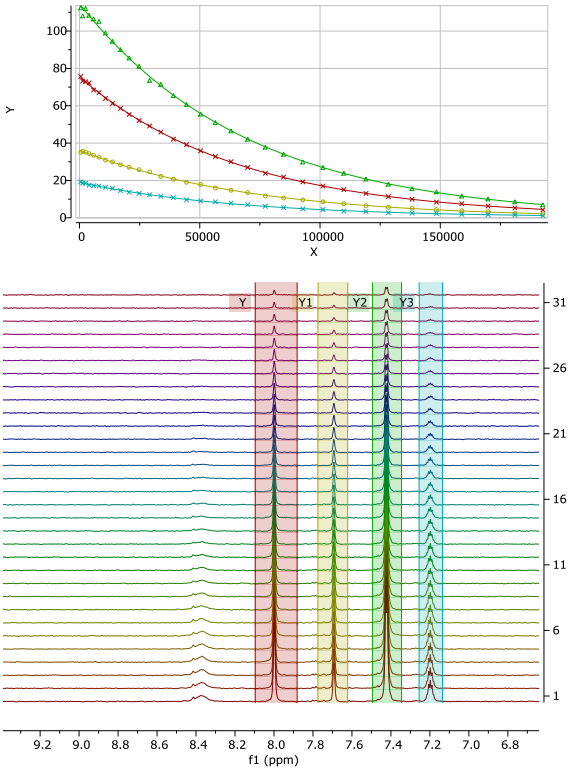

Receptor 3

D = 1,45e-5 (2e-7) cm2/s

Y' = B+F*exp(-X*G)
B=0.2046; F=75.24; G=0.00001483;
Error: 1.036e-7

Y1' = B+F*exp(-X*G)
B=-0.2697; F=36.47; G=0.00001404;
Error: 1.465e-7

Y2' = B+F*exp(-X*G)
B=-0.3623; F=115.0; G=0.00001422;
Error: 2.082e-7

Y3' = B+F*exp(-X*G)
B=0.1542; F=18.84; G=0.00001487;
Error: 2.110e-7

Figure S16. Analysis of the diffusion coefficient for receptor **3** with 1 eq. of KPF_6.

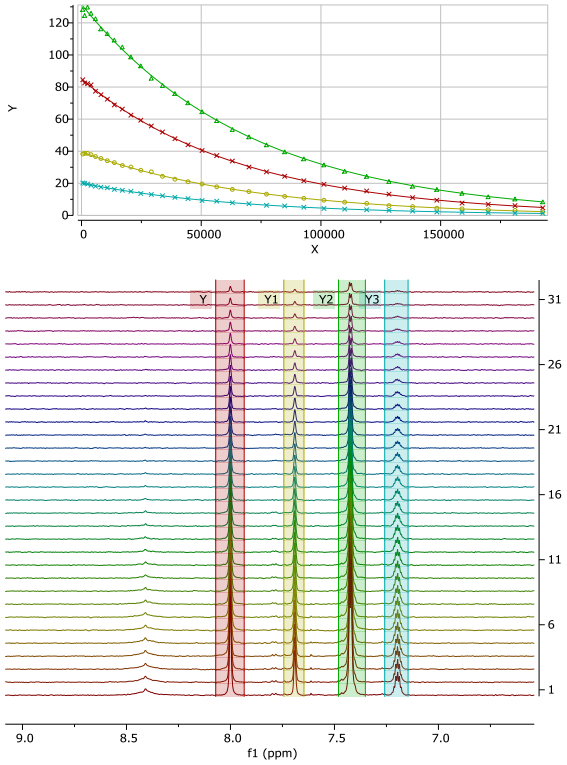

Receptor 3 + KPF6 [1 eq.]

D = 1,44e-5 (2e-7) cm2/s

Y' = B+F*exp(-X*G)
B=-0.1392; F=85.09; G=0.00001464;
Error: 9.421e-8

Y1' = B+F*exp(-X*G)
B=-0.4461; F=40.07; G=0.00001383;
Error: 1.622e-7

Y2' = B+F*exp(-X*G)
B=-0.3866; F=131.9; G=0.00001405;
Error: 1.953e-7

Y3' = B+F*exp(-X*G)
B=0.09421; F=20.02; G=0.00001495;
Error: 1.744e-7

Figure S17. Analysis of the diffusion coefficient for receptor **3** with 0.25 eq. of TBA_2SO_4.

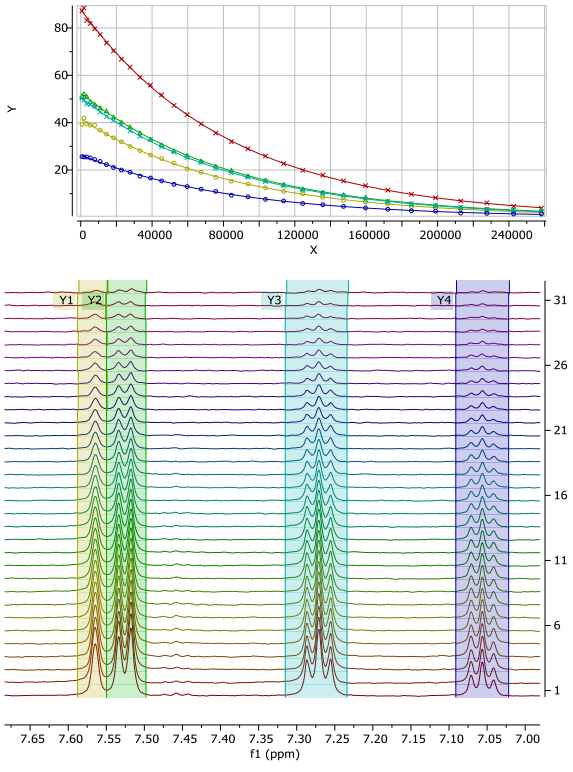

Receptor 3 + TBA2SO4 [0.25 eq.]

D = 1,174e-5 (1e-7) cm2/s

Y' = B+F*exp(-X*G)
B=-0.09250; F=88.00; G=0.00001185;
Error: 1.012e-7

Y1' = B+F*exp(-X*G)
B=-0.04413; F=41.58; G=0.00001162;
Error: 1.910e-7

Y2' = B+F*exp(-X*G)
B=-0.02277; F=52.60; G=0.00001169;
Error: 1.006e-7

Y3' = B+F*exp(-X*G)
B=-0.1936; F=50.81; G=0.00001161;
Error: 9.026e-8

Y4' = B+F*exp(-X*G)
B=-0.007203; F=26.42; G=0.00001195;
Error: 1.358e-7

Figure S18. Analysis of the diffusion coefficient for receptor **3** with 1 eq. of TBA_2SO_4.

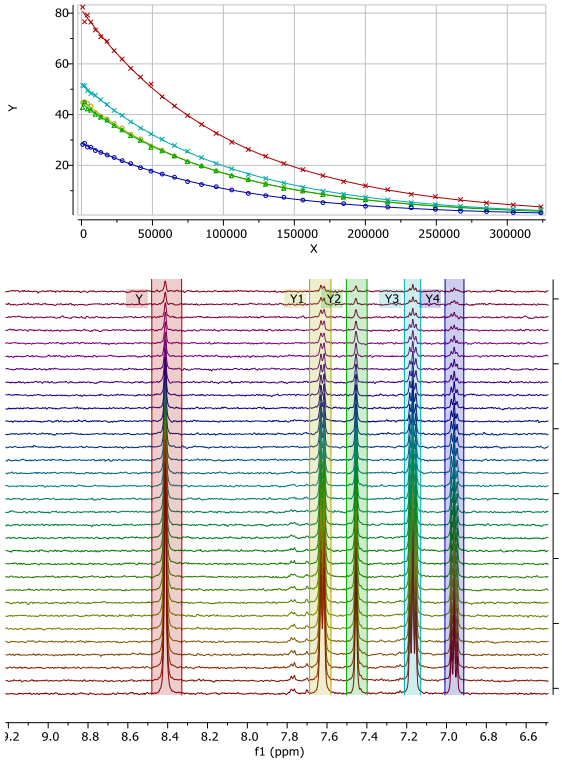

Receptor 3 + TBA2SO4 [1 eq.]

D = 0,97e-5 (1e-7) cm2/s

Y' = B+F*exp(-X*G)
B=-0.03587; F=81.32; G=0.000009569;
Error: 1.139e-7

Y1' = B+F*exp(-X*G)
B=0.3698; F=45.36; G=0.00001009;
Error: 8.513e-8

Y2' = B+F*exp(-X*G)
B=-0.1091; F=44.59; G=0.000009616;
Error: 1.143e-7

Y3' = B+F*exp(-X*G)
B=-0.1026; F=52.21; G=0.000009659;
Error: 5.978e-8

Y4' = B+F*exp(-X*G)
B=0.02699; F=28.74; G=0.000009774;
Error: 9.293e-8

Figure S19. Analysis of the diffusion coefficient for receptor **3** with 1 eq. of KPF_6 and 0.25 eq. of TBA_2SO_4.

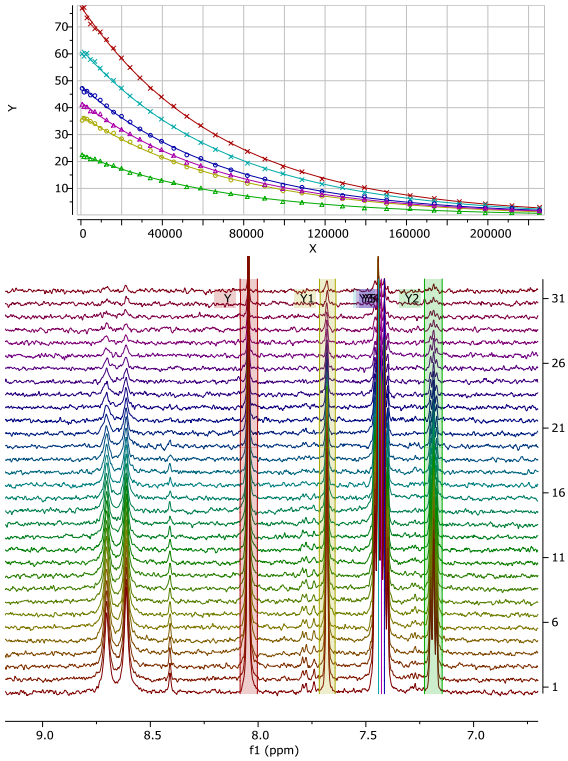

Receptor 3 + K [1 eq.] + TBA2SO4 [0.25eq]

D = 1.39e-5 (2e-7) cm2/s

Y' = B+F*exp(-X*G)
B=-0.3539; F=77.91; G=0.00001430;
Error: 1.181e-7

Y1' = B+F*exp(-X*G)
B=-0.5785; F=37.60; G=0.00001326;
Error: 1.921e-7

Y2' = B+F*exp(-X*G)
B=-0.2414; F=23.00; G=0.00001393;
Error: 1.841e-7

Y3' = B+F*exp(-X*G)
B=-0.5085; F=62.40; G=0.00001376;
Error: 1.398e-7

Y4' = B+F*exp(-X*G)
B=-0.1396; F=48.25; G=0.00001410;
Error: 1.618e-7

Y5' = B+F*exp(-X*G)
B=-0.1791; F=42.23; G=0.00001397;
Error: 1.465e-7

2D NMR

Figure S20. The ROESY NMR spectrum of receptor **1** with 0.5 eq. of K^+ and 0.25 eq. of SO_4^{2-}: a) aromatic protons range, b) squaramide protons range. The blue cross peaks describes the exchange peaks.

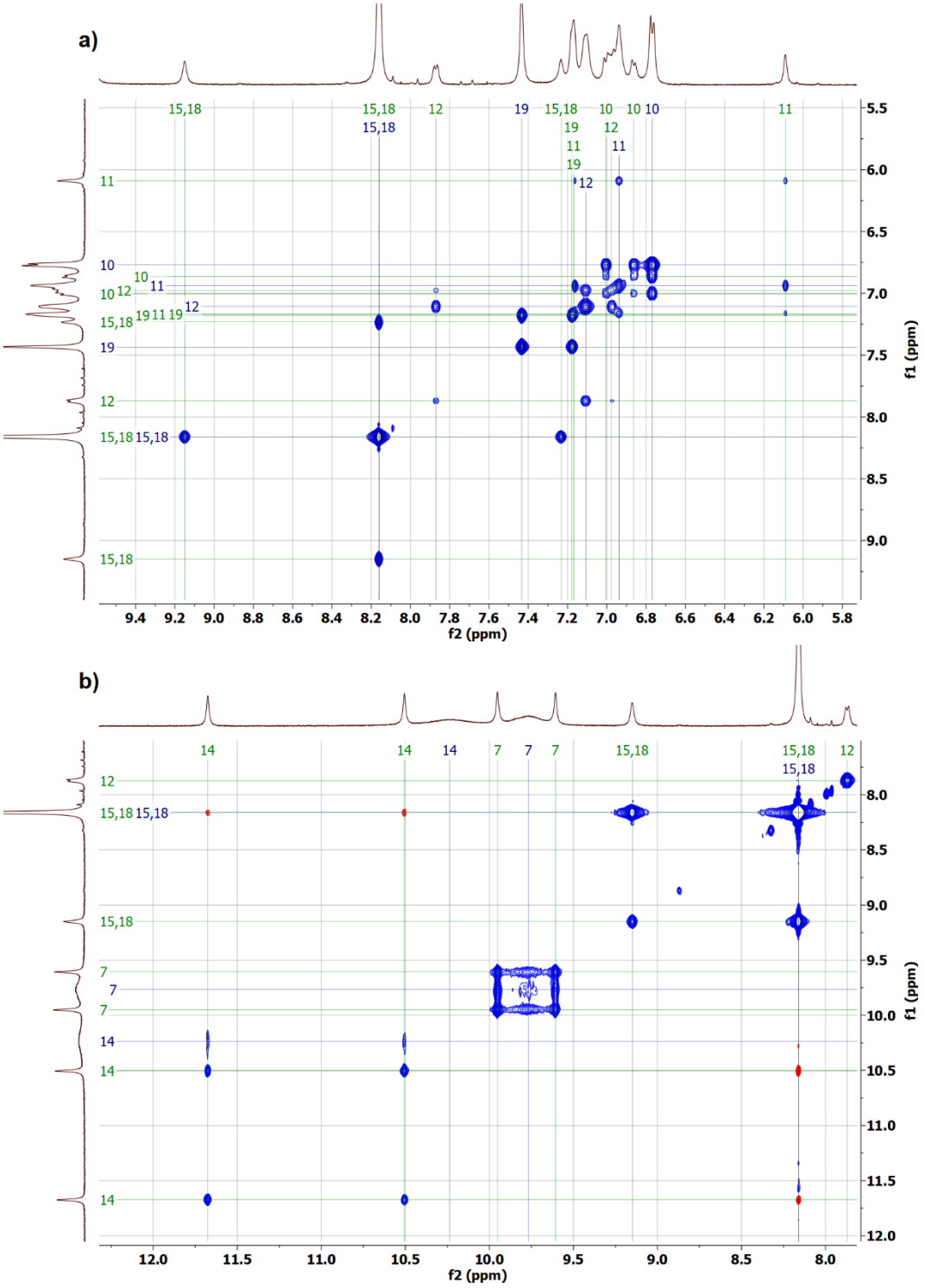

Figure S21. The aromatic part of the HSQC NMR spectrum of receptor **1** with 0.5 eq. of K^+ and 0.25 eq. of SO_4^{2-}.

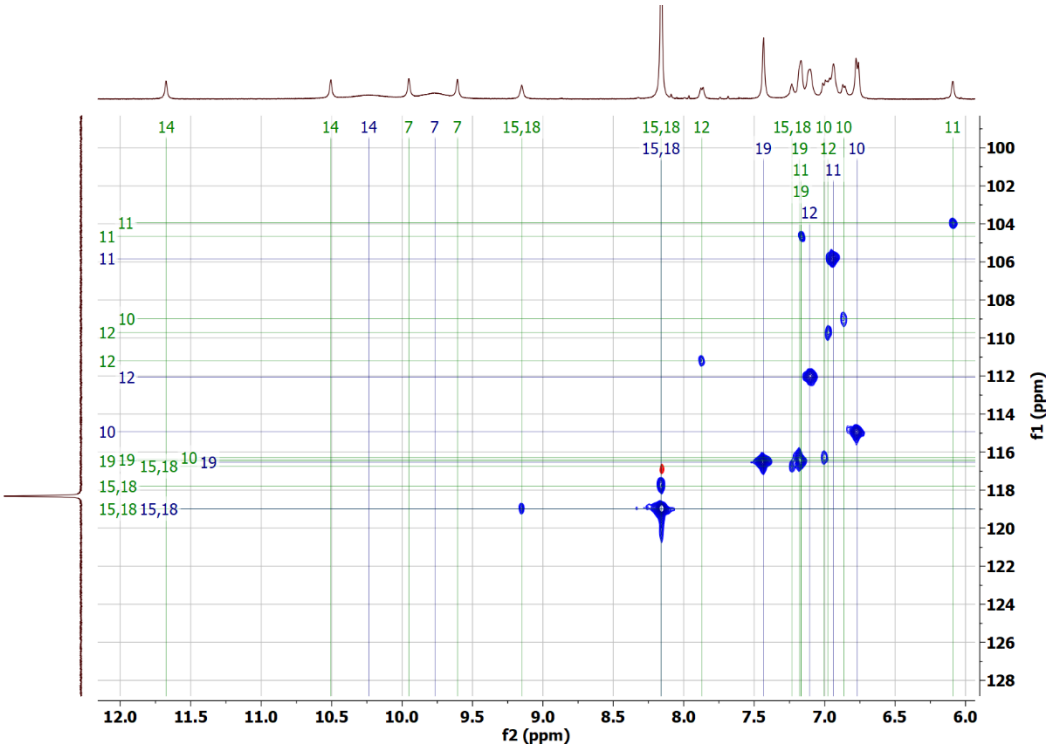

EXTRACTION EXPERIMENT (SLE)

The solid–liquid extraction (SLE) experiments were carried out at 298 K in acetonitrile, using the same receptor concentration as in the ^{1}H NMR titrations. In a 2 mL vial, 1.0 mL of a freshly prepared ca. 3 mM solution of the receptor in CH_3CN was combined with an excess of the solid sulfate salt (Na_2SO_4 or K_2SO_4). The suspension was stirred for 1 h at room temperature, then the supernatant was collected and passed through a 0.20 µm PTFE syringe filter. An aliquot (500 µL) of the filtrate was transferred to a 5 mm NMR tube and the ^{1}H NMR spectrum was acquired on a Bruker 300 spectrometer at 298 K.

HYDRODYNAMIC RADII

The hydrodynamic radii (Stokes radii) were calculated using the SEGWE calculator [10], based on measured diffusion coefficients presented in Table 1 in the main text.

Table S1. Hydrodynamic radius, r_H (10^{-12} m), for receptors **1-3** and their various complexes in CD_3CN solutions.

	1	**2**	**3**
free receptor	707	731	599
1 eq. KPF_6	804	757	602
0.25 eq. TBA_2SO_4	817	891	702
1 eq. TBA_2SO_4	935	1018	811
1 eq. KPF_6 0.25 eq. TBA_2SO_4	926 and 1029*	867	618

* Value for the second component.

CRYSTAL DATA

[1×KPF_6]

Single crystals suitable for X-ray diffraction analysis were obtained as follows. An equimolar amount of KPF_6 was added to an acetonitrile solution of the receptor. The resulting solution was stirred until complete dissolution and equilibration. It was then filtered through a syringe filter to remove any potential insoluble impurities. The clear filtrate was subjected to slow vapor diffusion of diethyl ether. Over time, this procedure afforded single crystals suitable for X-ray analysis. A representative crystal was selected for structural determination.

A pale yellow, lathshaped specimen of $C_{57.10}H_{58.25}F_{18}KN_{5.25}O_{14.65}P$, approximate dimensions 0.047×0.072×0.36 mm^3, was used for the Xray crystallographic analysis. The X-ray intensity data of SQP5_KPF6 were measured on a Bruker D8 VENTURE Bruker D8 VENTURE system equipped with an INCOATEC I\mS micro-focus source (CuK_α radiation, λ = 1.54178 Å) and a HELIOS multilayer optics monochromator. The specimen was held at 130(1) K during the measurement with an Oxford Cryostream 1000 low temperature device. A total of 6593 frames were collected with APEX3 program[1]. The total exposure time was 41.77 hours. The frames were integrated with the SAINT V8.41 package using a narrow-frame algorithm[2]. The integration of the data using a triclinic unit cell yielded a total of 43857 reflections to a maximum θ angle of 66.50° (0.84 Å resolution), of which 10906 were independent (average redundancy 4.02, completeness = 98.5%, R_{int} = 2.69%, R_{sig} = 1.97%) and 10323 (94.7%) were greater than 2σ(F^2). The final cell constants of a = 11.8115(3) Å, b = 14.1038(4) Å, c = 20.1361(5) Å, α = 70.0540(10)°, β = 88.1140(10)°, γ = 85.5820(10)°, V = 3143.75(14) $Å^3$, are based upon the refinement of the XYZcentroids of 9730 reflections above 20 σ(I) with 4.67° < 2θ < 133.27°. Data were corrected for absorption effects using the Multi-Scan method in SADABS 2016/2[3]. The ratio of minimum to maximum apparent transmission yields 0.843. The calculated minimum and maximum transmission coefficients (based on crystal size) are 0.521 and 0.908[4].

The structure was solved by Intrinsic Phasing methods with SHELXS-2013/1 and refined by fullmatrix least squares methods against F^2 using SHELXL-2018/3 in the space group $P\bar{1}$, with Z = 2 for the formula unit $C_{57.10}H_{58.25}F_{18}KN_{5.25}O_{14.65}P$ corresponding to: $C_{52}H_{48}F_{12}KN_4O_{14}^+ + PF_6^- + 0.65\times C_4H_{10}O + 1.25\times CH_3CN$[5,6]. The final anisotropic full-matrix least-squares refinement on F^2 with 951 variables against 10906 data points and 113 restraints converged at R_1 = 5.29%, for the observed 10323 data with [$I \geq 2\sigma(I)$] and wR_2 = 14.15% for all data. The goodness-of-fit on F^2 was 1.04. The largest peak in the final difference electron density synthesis was 0.66 $e^-/Å^3$ and the deepest hole was −0.65 $e^-/Å^3$ with an RMS deviation of 0.062 $e^-/Å^3$. On the basis of the final model, the calculated density was 1.55 g/cm^3 and F(000), 1502 e^-. Crystal data and refined structure parameters are presented in Table S2.

Disorder description

The structure is disordered and contains all four CF_3 groups disordered over alternative positions. The CF_3 group at C25 atom is disordered over two positions with fixed occupancy ratio of 0.8:0.2. The CF_3 group at C26 atom is disordered over two positions with fixed occupancy ratio of 0.6:0.4. The CF_3 group at C51 atom is disordered over three positions with fixed occupancy ratio of 0.5:0.3:0.2. The CF_3 group at C52 atom is disordered over two positions with fixed occupancy ratio of 0.8:0.2. In addition, the structure contains one full-occupancy ordered acetonitrile molecule and non-stoichiometric amount of disordered diethyl ether and acetonitrile moieties sharing common site with fixed occupancy ratio of 0.45:0.2:0.25 for Et_2O:Et_2O:CH_3CN fragments respectively. To preserve reasonable geometry of the disorder molecular fragments a number of distance and angle restraints was used together with restraints for atomic displacement parameters.

Structure refinement details

All ordered and main component disordered (sum occupancy ≥0.5) non-hydrogen atoms were refined with anisotropic displacement parameters. All hydrogen atoms were refined isotropic on calculated positions using a riding model with their U_{iso} values constrained to 1.5 times the U_{eq} of their pivot atoms for terminal sp^3 carbon atoms and 1.2 times for all other carbon atoms.
For the model building and the structure refinement the ShelXle graphical user interface was employed[7]. This report was generated using FinalCif[8]. Molecular graphics was prepared using program Mercury 2024.3.0[9]. Thermal ellipsoids parameters are presented at 50% probability level in Figure S22, whereas packing diagrams are displayed in Figure S23.

Table S2. Crystal data and structure refinement for **1×KPF$_6$**

Empirical formula	$C_{57.10}H_{58.25}F_{18}KN_{5.25}O_{14.65}P$ corresponding to: $C_{52}H_{48}F_{12}KN_4O_{14}^+ + PF_6^- + 0.65\times C_4H_{10}O + 1.25\times CH_3CN$
M_x [g·mol^{-1}]	1464.51
T [K]	130(1)
Radiation	CuK_α (λ = 1.54178 Å)
Crystal size [mm^3]	0.047×0.072×0.36
Crystal habit	pale yellow lath
Crystal system	triclinic
Space group (number)	$P\bar{1}$ (2)
Unit cell parameters	a = 11.8115(3) Å α = 70.0540(10)° b = 14.1038(4) Å β = 88.1140(10)° c = 20.1361(5) Å γ = 85.5820(10)°
V [Å^3], Z	3143.75(14), 2
D_x [g·cm^{-3}]	1.547
μ [mm^{-1}]	2.085
F(000)	1502
$2\theta_{min}$, $2\theta_{max}$	4.67°, 133.00° (0.84 Å resolution)
Index ranges	−13 ≤ h ≤ 14 −16 ≤ k ≤ 16 −23 ≤ l ≤ 23
Reflections collected/ independent	43857 / 10906 (R_{int} = 0.0269, R_{sig} = 0.0197)
Completeness to $2\theta_{max}$ = 133.00°	98.5%
Absorption correction	Multi-Scan
T_{min}, T_{max}	0.521, 0.908
Refinement method	full-matrix LSQ on F^2
Data / Restraints / Parameters	10906 / 113 / 951
GOF on F^2	1.039
Final R indexes	10323 data R_1 = 0.0529, wR_2 = 0.1397 all data R_1 = 0.0549, wR_2 = 0.1415
$\Delta\rho_{max}$, $\Delta\rho_{min}$	0.66 e/Å^{-3}, −0.65 e/Å^{-3}

Figure S22. Thermal ellipsoid plot for **1×KPF$_6$** at the 50% probability level. Hydrogen atoms and solvent molecules omitted. Selected atoms labelled only.

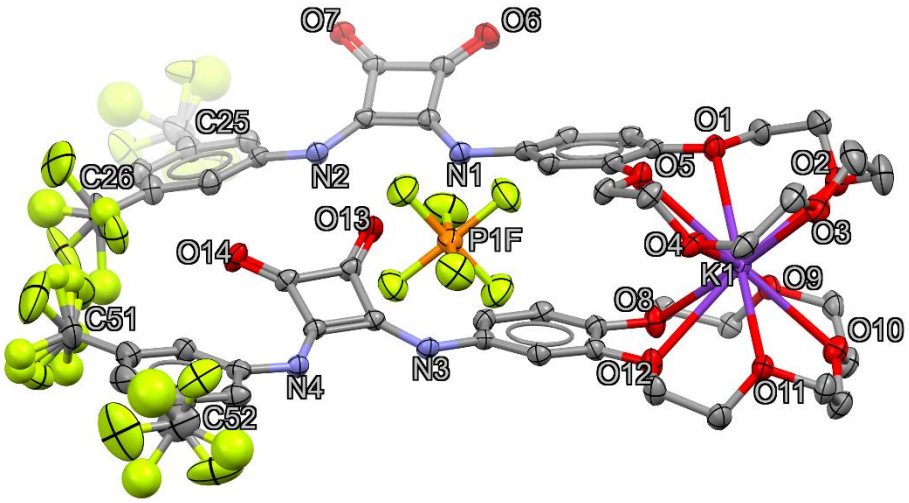

Figure S23. Packing diagram for **1×KPF$_6$**, view along [100] a), [010] b) and [001] c). Hydrogen atoms omitted. K^+ complexed by crown ether moieties and PF_6^- ions depicted as polyhedra.

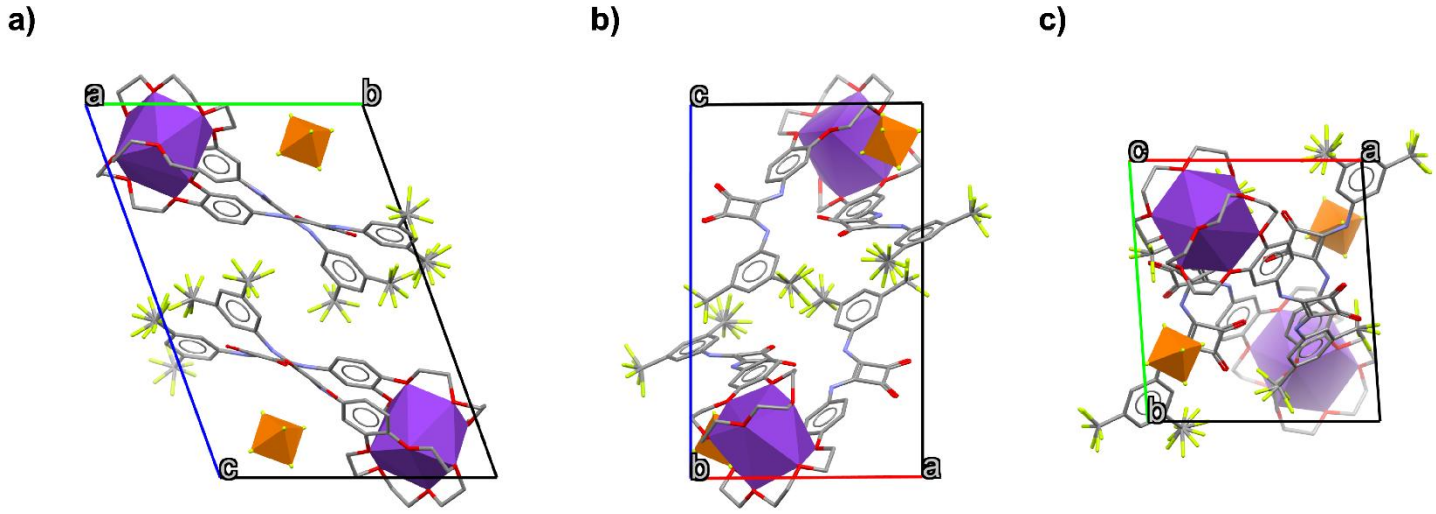

[1×KCl]

Single crystals suitable for X-ray diffraction analysis were obtained as follows. An acetonitrile solution of the receptor was saturated with KCl under solid–liquid extraction conditions. After equilibration, the suspension was filtered through a syringe filter to remove any undissolved solids. The resulting clear solution was then subjected to slow vapor diffusion of diethyl ether. Over time, this procedure yielded single crystals suitable for X-ray analysis. A representative crystal was selected for structural determination.

A clear pale-yellow, plate-shaped specimen of $C_{54}H_{53}ClF_{12}KN_5O_{15}$, approximate dimensions 0.046×0.143×0.245 mm^3, was used for the X-ray crystallographic analysis. The X-ray intensity data of **1×KCl** were measured on a Bruker D8 VENTURE Bruker D8 VENTURE system equipped with an INCOATEC I\mS

micro-focus source (CuK_α radiation, λ = 1.54178 Å) and a HELIOS multilayer optics monochromator. The specimen was held at 130(1) K during the measurement with a low temperature device.
A total of 6072 frames were collected with APEX3 program[1]. The total exposure time was 63.22 hours. The frames were integrated with the SAINT V8.41 package using a narrow-frame algorithm[2]. The integration of the data using a monoclinic unit cell yielded a total of 89010 reflections to a maximum θ angle of 67.98° (0.83 Å resolution), of which 10521 were independent (average redundancy 8.46, completeness = 100.0%, R_{int} = 4.38%, R_{sig} = 1.98%) and 9740 (92.6%) were greater than 2σ(F^2). The final cell constants of a = 11.6788(3) Å, b = 40.5906(10) Å, c = 12.3583(3) Å, α = 90°, β = 99.2020(10)°, γ = 90°, V = 5783.1(2) Å^3, are based upon the refinement of the XYZ-centroids of 9563 reflections above 20 σ(I) with 7.57° < 2θ < 136.39°. Data were corrected for absorption effects using the Multi-Scan method in SADABS 2016/2[3]. The ratio of minimum to maximum apparent transmission yields 0.768. The calculated minimum and maximum transmission coefficients (based on crystal size) are 0.614 and 0.905[4].
The structure was solved by Intrinsic Phasing methods with SHELXT-2018/2 and refined by full-matrix least-squares methods against F^2 using SHELXL-2018/3 in the space group $P2_1/n$, with Z = 4 for the formula unit $C_{54}H_{53}ClF_{12}KN_5O_{15}$ corresponding to: $C_{52}H_{48}F_{12}KN_4O_{14}^+ + CH_3CN + Cl^- + H_2O$[5,6]. The final anisotropic full-matrix least-squares refinement on F^2 with 874 variables against 10521 data points and 45 restraints converged at R_1 = 3.40%, for the observed 9740 data with [$I \geq 2\sigma(I)$] and wR_2 = 8.81% for all data. The goodness-of-fit on F^2 was 1.05. The largest peak in the final difference electron density synthesis was 0.32 e$^-$/Å^3 and the deepest hole was −0.24 e$^-$/Å^3 with an RMS deviation of 0.040 e$^-$/Å^3. On the basis of the final model, the calculated density was 1.51 g/cm^3 and F(000), 2704 e$^-$. Crystal data and refined structure parameters are presented in **Table S3**.

Disorder description

The structure is disordered and contains O-CH_2-CH_2-O moiety in one of the crown ethers located at two sites with refined occupancy ratio yielding 0.879(5):0.121(5). In addition, three CF_3 groups are disordered over two positions each as well. The refined occupancy ratio for CF_3 moieties converged to 0.914(8):0.086(8), 0.941(3):0.059(3) and 0.919(8):0.081(8) for C26/C26B, C51/C51B and C52/C52B atoms respectively which are common for alternative fragments. To preserve reasonable geometry of the disorder molecular fragments a number of distance and angle restraints was used together with restraints for atomic displacement parameters.

Structured refinement details

All ordered and main component disordered (sum occupancy > 0.8) non-hydrogen atoms were refined with anisotropic displacement parameters. All hydrogen atoms were refined with isotropic displacement parameters. Some of their coordinates of most of the H atomoms were refined on calculated positions using a riding model with their U_{iso} values constrained to 1.5 times the U_{eq} of their pivot atoms for terminal sp^3 carbon atoms and 1.2 times for all other carbon atoms. Coordinates of H atoms of N-H and H_2O moieties were refined freely together with the U_{iso} parameters.
For the model building and the structure refinement the ShelXle graphical user interface was employed[7]. This report was generated using FinalCif[8]. Molecular graphics was prepared using program Mercury 2024.3.0[9]. Thermal ellipsoids parameters are presented at 50% probability level in Figure S24, whereas packing diagrams are displayed in Figure S25.

Table S3. Crystal data and structure refinement for **1×KCl**

Empirical formula	$C_{54}H_{53}ClF_{12}KN_5O_{15}$ corresponding to: $C_{52}H_{48}F_{12}KN_4O_{14}^+ + CH_3CN + Cl^- + H_2O$
M_x [g·mol^{-1}]	1314.56
T [K]	130(1)
Radiation	CuK_α (λ = 1.54178 Å)
Crystal size [mm^3]	0.046×0.143×0.245
Crystal habit	clear pale-yellow plate
Crystal system	monoclinic
Space group (number)	$P2_1/n$ (14)
Unit cell parameters	a = 11.6788(3) Å α = 90° b = 40.5906(10) Å β = 99.2020(10)° c = 12.3583(3) Å γ = 90°
V [Å^3], Z	5783.1(2), 4
D_x [g·cm^{-3}]	1.51
μ [mm^{-1}]	2.209
F(000)	2704
$2\theta_{min}$, $2\theta_{max}$	4.35°, 135.97° (0.83 Å resolution)
Index ranges	−14 ≤ h ≤ 14 −48 ≤ k ≤ 48 −14 ≤ l ≤ 14
Reflections collected/ independent	89010 / 10521 (R_{int} = 0.0438, R_{sig} = 0.0198)
Completeness to $2\theta_{max}$ = 135.97°	100.0%
Absorption correction	Multi-Scan
T_{min}, T_{max}	0.614, 0.905
Refinement method	full-matrix LSQ on F^2
Data / Restraints / Parameters	10521 / 45 / 874
GOF on F^2	1.055
Final R indexes	9740 data R_1 = 0.0340, wR_2 = 0.0861 all data R_1 = 0.0367, wR_2 = 0.0881
$\Delta\rho_{max}$, $\Delta\rho_{min}$	0.32 e/Å^{-3}, −0.24 e/Å^{-3}

Figure S24. Thermal ellipsoid plot for **1×KCl** at the 50% probability level. C-H Hydrogen atoms omitted. Selected atoms labbeled only.

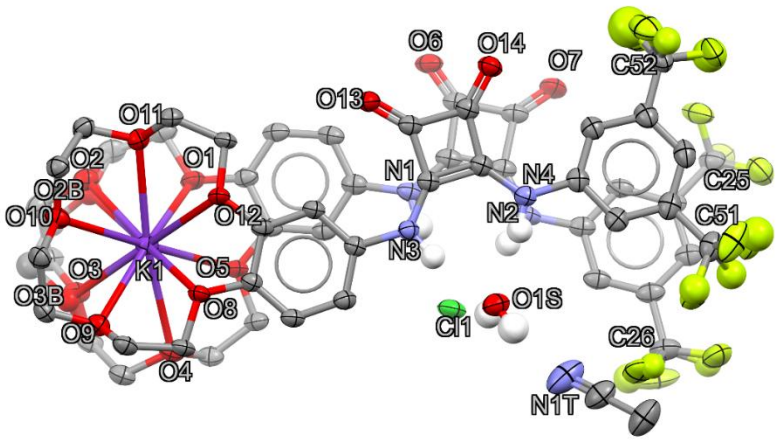

Figure S25. Packing diagram for **1×KCl**, view along [100] a), [010] b) and [001] c). Hydrogen atoms omitted. K^+ complexed by crown ether moieties depicted as polyhedra.

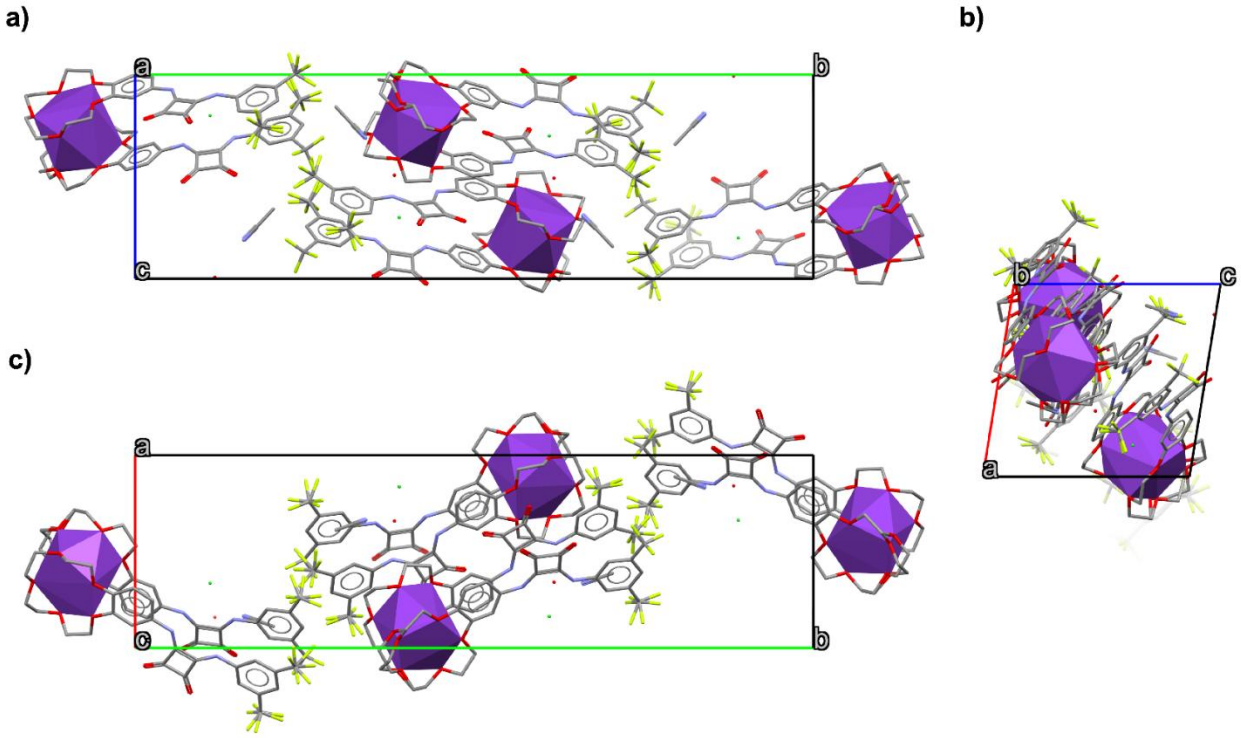

[1×K_2SO_4]

Single crystals suitable for X-ray diffraction analysis were obtained as follows. An acetonitrile solution of the receptor was saturated with K_2SO_4 under solid–liquid extraction conditions. After equilibration, the suspension was filtered through a syringe filter to remove any undissolved solids. The resulting clear solution was then subjected to slow vapor diffusion of diethyl ether. Over time, this procedure yielded single crystals suitable for X-ray analysis. A representative crystal was selected for structural determination.

A clear colourless, block-shaped specimen of $C_{115.05}H_{112.57}F_{24}K_2N_{13.52}O_{32}S$, approximate dimensions 0.16×0.194×0.542 mm^3, was used for the X-ray crystallographic analysis. The X-ray intensity data of **1×K_2SO_4** were measured on a Bruker D8 VENTURE Bruker D8 VENTURE system equipped with a fine focus sealed tube (MoK_α radiation, λ = 0.71073 Å) and a HELIOS multilayer optics monochromator. The specimen was held at 130(1) K during the measurement with a low temperature device.
A total of 2394 frames were collected with APEX3 program[1]. The total exposure time was 20.07 hours. The frames were integrated with the SAINT V8.41 package using a narrow-frame algorithm[2]. The integration of the data using a triclinic unit cell yielded a total of 243001 reflections to a maximum θ angle of 25.02° (0.84 Å resolution), of which 44708 were independent (average redundancy 5.44, completeness = 99.8%, R_{int} = 3.89%, R_{sig} = 3.14%) and 39063 (87.4%) were greater than 2σ(F^2). The final cell constants of a = 20.0763(19) Å, b = 20.094(2) Å, c = 32.699(3) Å, α = 87.699(4)°, β = 87.562(3)°, γ = 74.488(3)°, V = 12693(2) $Å^3$, are based upon the refinement of the XYZ-centroids of 9729 reflections above 20 σ(I) with 5.74° < 2θ < 53.49°. Data were corrected for absorption effects using the Multi-Scan method in SADABS 2016/2[3]. The ratio of minimum to maximum apparent transmission yields 0.883. The calculated minimum and maximum transmission coefficients (based on crystal size) are 0.896 and 0.968[4].

The structure was solved by Intrinsic Phasing methods with SHELXS-2013/1 and refined by full-matrix least-squares methods against F^2 using SHELXL-2018/3 in the space group $P\bar{1}$, with Z = 4 for the formula unit $C_{115.05}H_{112.57}F_{24}K_2N_{13.52}O_{32}S$ corresponding to: $2\times C_{52}H_{48}F_{12}KN_4O_{14}^- + SO_4^{2-} + 5.525\times CH_3CN$[5,6]. The final anisotropic full-matrix least-squares refinement on F^2 with 3678 variables against 44708 data points and 350 restraints converged at R_1 = 4.36%, for the observed 39063 data with [$I \geq 2\sigma(I)$] and wR_2 = 11.43% for all data. The goodness-of-fit on F^2 was 1.06. The largest peak in the final difference electron density synthesis was 0.53 $e^-/Å^3$ and the deepest hole was −0.47 $e^-/Å^3$ with an RMS deviation of 0.054 $e^-/Å^3$. On the basis of the final model, the calculated density was 1.45 g/cm^3 and F(000), 5694 e^-. Crystal data and refined structure parameters are presented in Table S4.

Disorder description

The unit cell in the asymmetric part contains: four receptor pairs, each pair joined by K^+ ion complexed by crown ether moieties, two SO_4^{2-} anions and 11.05 acetonitrile solvent molecules. The structure is disordered and contains C_{ar}-O-CH_2-CH_2-O-CH_2-CH_2-O-CH_2-CH_2-O moiety in one of the crown ethers in moiety A located at two sites with fixed occupancy ratio of 0.8:0.2. In addition, several CF_3 groups are disordered. In the moiety A CF_3 group at C25 atom is disordered over three positions with fixed occupancy ratio of 0.5:0.4:0.1, whereas CH_3 group at C26 atom is disordered over two positions with fixed occupancy ratio of 0.6:0.4. In the moiety B CF_3 group at C52 atom is disordered over two positions with fixed occupancy ratio of 0.85:0.15. In the moiety C CF_3 group at C26 atom is disordered over three positions with fixed occupancy ratio of 0.5:0.5. In the moiety D CF_3 group at C26 atom is disordered over three positions with fixed occupancy ratio of 0.5:0.3:0.2. The crystal contains also non-stoichiometric amount of CH_3CN solvent molecules some of them disordered over multiple positions. To preserve reasonable geometry of the disorder molecular fragments a number of distance and angle restraints was used together with restraints for atomic displacement parameters.

Structured refinement details

All ordered and main component disordered (sum occupancy ≥0.5) non-hydrogen atoms were refined with anisotropic displacement parameters. All hydrogen atoms were refined with isotropic displacement parameters. Some of their coordinates of most of the H atoms were refined on calculated positions using a riding model with their U_{iso} values constrained to 1.5 times the U_{eq} of their pivot atoms for terminal sp^3 carbon atoms and 1.2 times for all other carbon atoms. Coordinates of H atoms of N-H and H_2O moieties were refined freely together with the U_{iso} parameters.
For the model building and the structure refinement the ShelXle graphical user interface was employed[7]. This report was generated using FinalCif[8]. Molecular graphics was prepared using program Mercury 2024.3.0[9]. Thermal ellipsoids parameters are presented at 50% probability level in **Figures S26-S29**, whereas packing diagrams are displayed in **Figure S30**.

Table S4. Crystal data and structure refinement for **1×K_2SO_4**

Empirical formula	$C_{115.05}H_{112.57}F_{24}K_2N_{13.52}O_{32}S$ corresponding to: $2\times C_{52}H_{48}F_{12}KN_4O_{14}^- + SO_4^{2-} + 5.525\times CH_3CN$
M_x [g·mol^{-1}]	2762.96
T [K]	130(1)
Radiation	MoK_α (λ = 0.71073 Å)
Crystal size [mm^3]	0.16×0.194×0.542
Crystal habit	clear colourless block
Crystal system	triclinic
Space group (number)	$P\bar{1}$ (2)
Unit cell parameters	a = 20.0763(19) Å α = 87.699(4)° b = 20.094(2) Å β = 87.562(3)° c = 32.699(3) Å γ = 74.488(3)°
V [Å^3], Z	12693(2), 4

D_x [g·cm^{-3}]	1.446
μ [mm^{-1}]	0.207
F(000)	5694
$2\theta_{min}$, $2\theta_{max}$	5.72°, 50.05° (0.84 Å resolution)
Index ranges	−23 ≤ h ≤ 23 −23 ≤ k ≤ 23 −38 ≤ l ≤ 38
Reflections collected/ independent	243001 / 44708 (R_{int} = 0.0389, R_{sig} = 0.0314)
Completeness to $2\theta_{max}$ = 50.05°	99.8%
Absorption correction	Multi-Scan
T_{min}, T_{max}	0.896, 0.968
Refinement method	full-matrix LSQ on F^2
Data / Restraints / Parameters	44708 / 350 / 3678
GOF on F^2	1.059
Final R indexes	39063 data: R_1 = 0.0436, wR_2 = 0.1038 all data: R_1 = 0.0559, wR_2 = 0.1143
$\Delta\rho_{max}$, $\Delta\rho_{min}$	0.53 e/Å^{-3}, −0.47 e/Å^{-3}
Extinction coefficient	0.00139(7)

Figure S26. Thermal ellipsoid plot for molecule A in **1×K_2SO_4** at the 50% probability level. Hydrogen atoms and solvent molecules omitted. Selected atoms labbeled only.

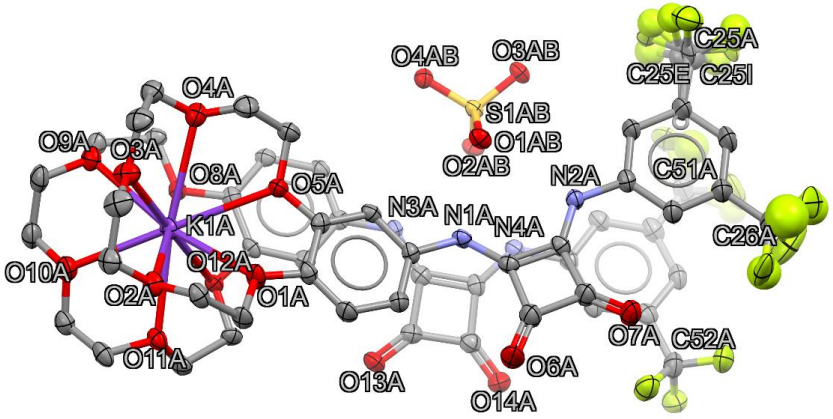

Figure S27. Thermal ellipsoid plot for molecule B in **1×K_2SO_4** at the 50% probability level. Hydrogen atoms and solvent molecules omitted. Selected atoms labbeled only.

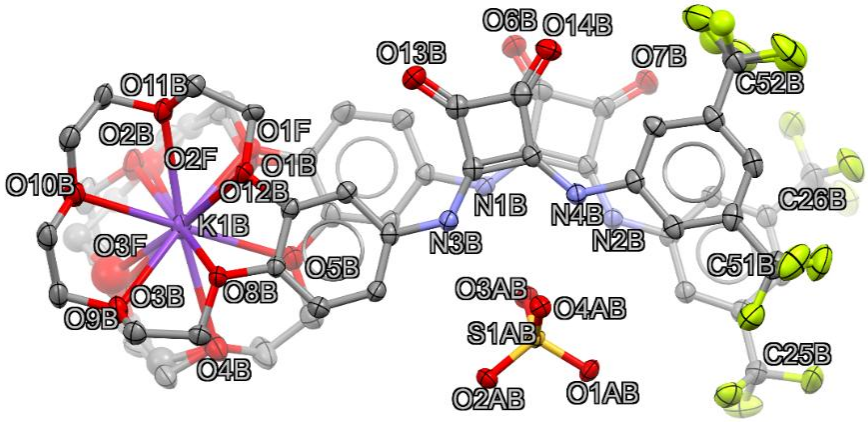

Figure S28. Thermal ellipsoid plot for molecule C in **1×K_2SO_4** at the 50% probability level. Hydrogen atoms and solvent molecules omitted. Selected atoms labbeled only.

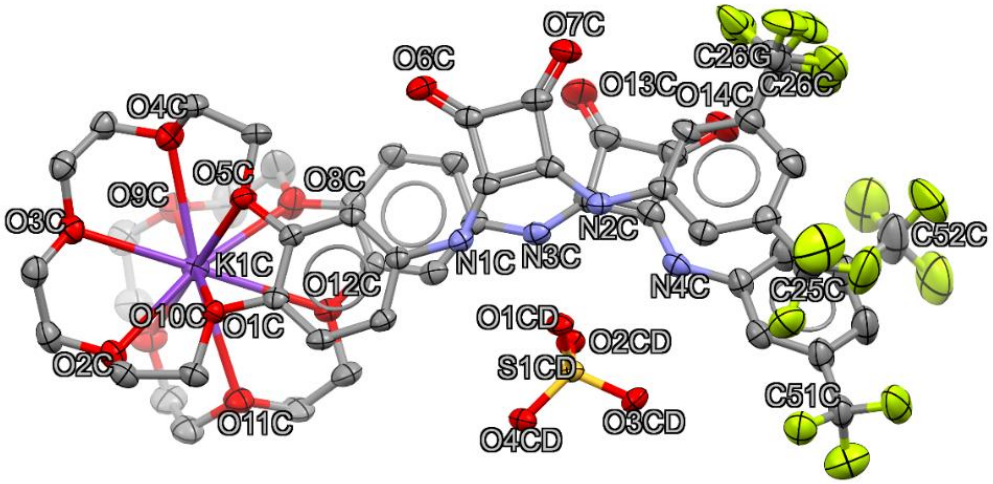

Figure S29. Thermal ellipsoid plot for molecule D in **1×K_2SO_4** at the 50% probability level. Hydrogen atoms and solvent molecules omitted. Selected atoms labbeled only.

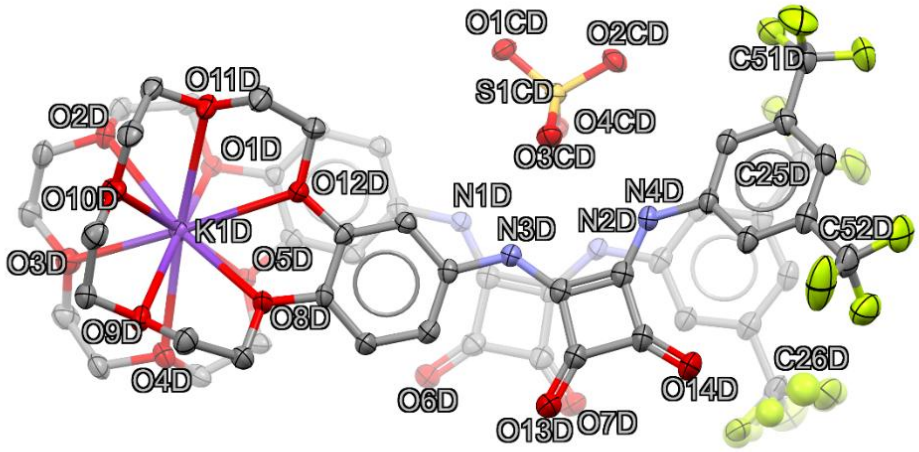

Figure S30. Packing diagram for **1×K_2SO_4**, view along [100] a), [010] b) and [001] c). Hydrogen atoms omitted. K^+ complexed by crown ether moieties and SO_4^{2-} ions depicted as polyhedra.

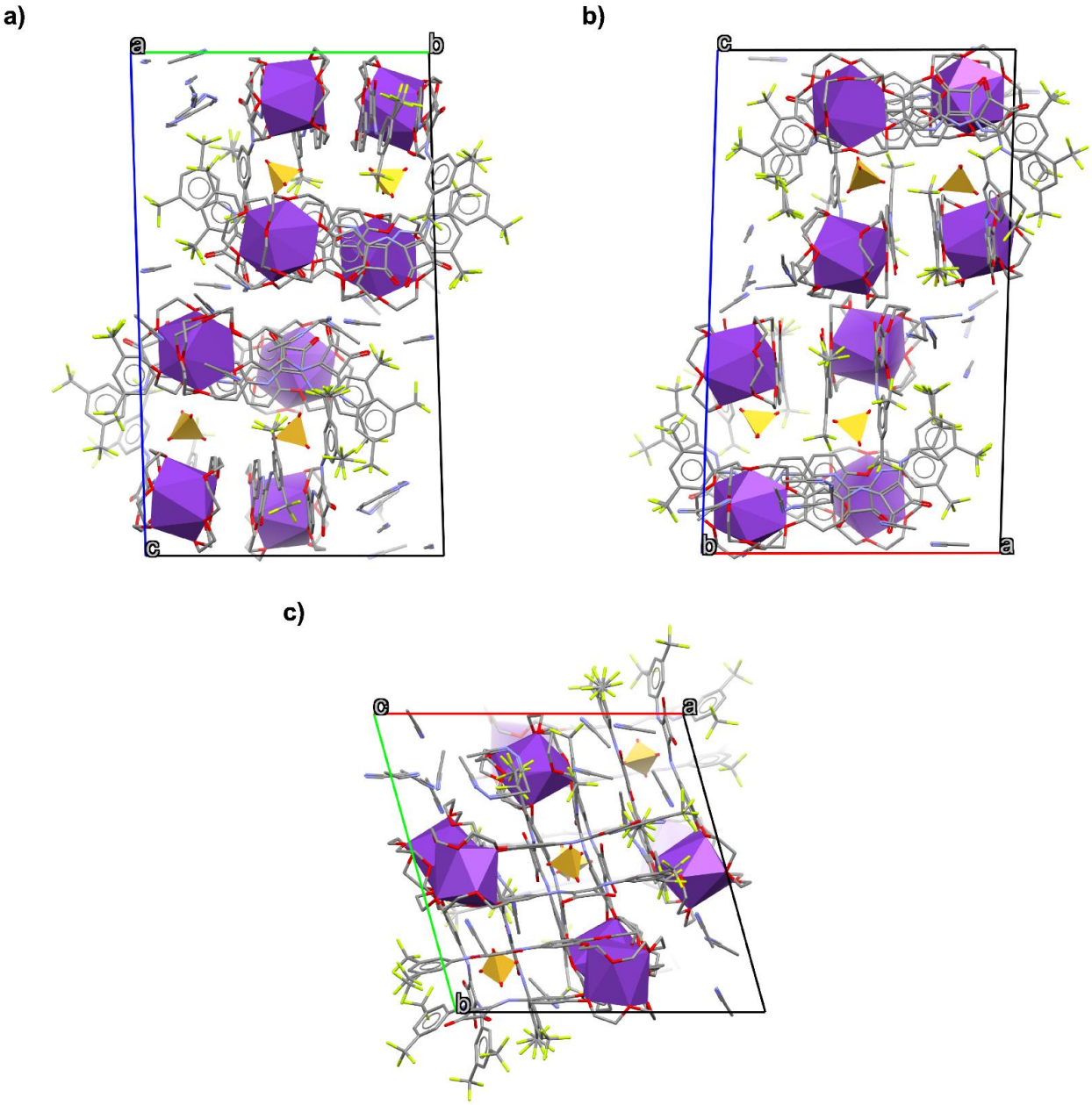

NMR SPECTRA

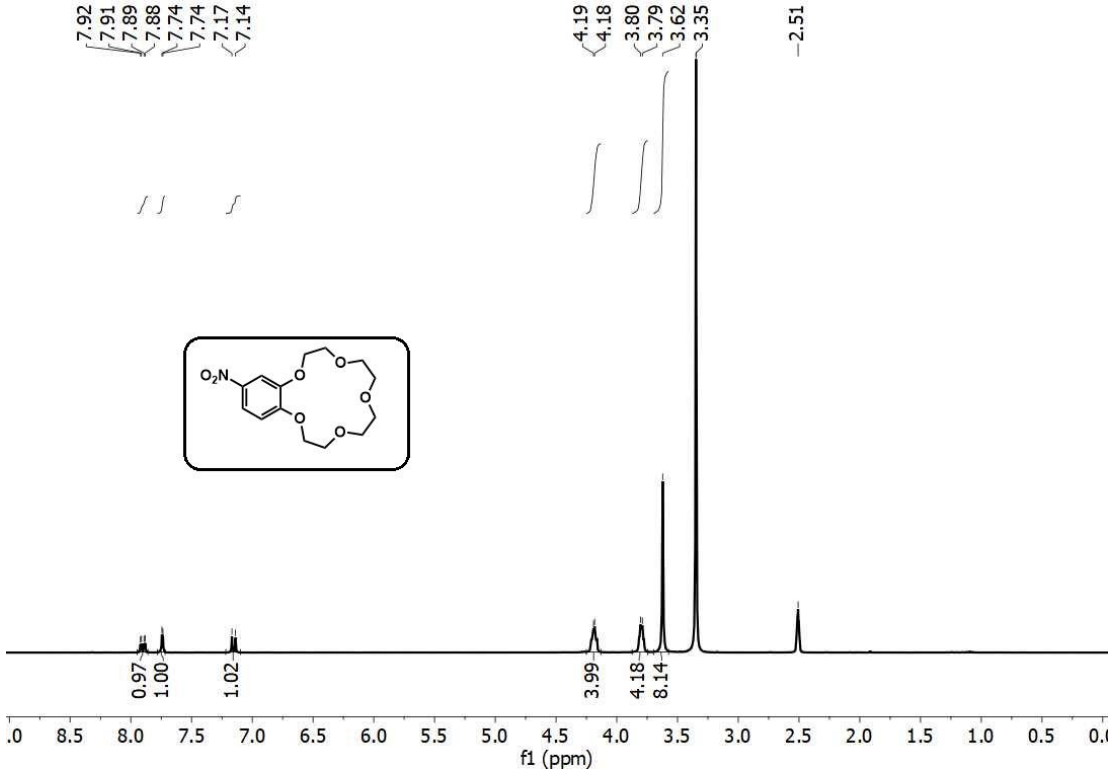
7.92
7.91
7.89
7.88
7.74
7.74
7.17
7.14
4.19
4.18
3.80
3.79
3.62
3.35
2.51
0.97
1.00
1.02
3.99
4.18
8.14
f1 (ppm)

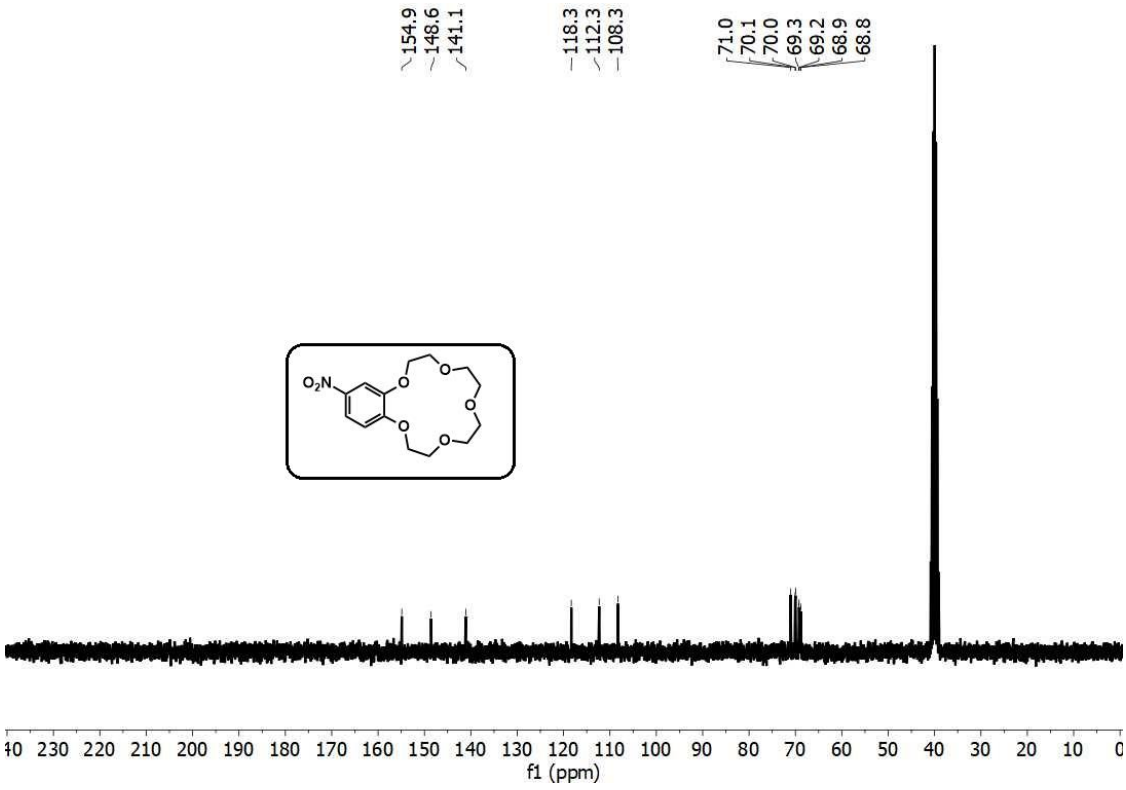
154.9
148.6
141.1
118.3
112.3
108.3
71.0
70.1
70.0
69.3
69.2
68.9
68.8
f1 (ppm)

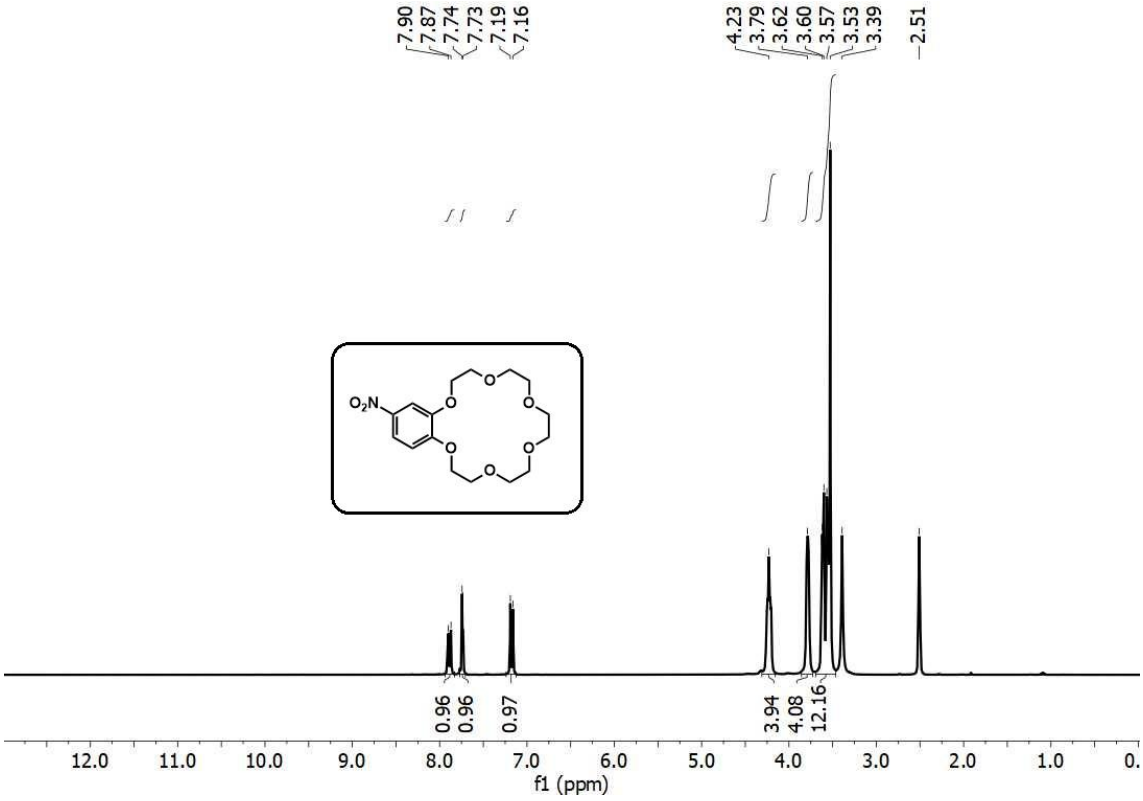
7.90
7.87
7.74
7.73
7.19
7.16
4.23
3.79
3.62
3.60
3.57
3.53
3.39
2.51
0.96
0.96
0.97
3.94
4.08
12.16
f1 (ppm)

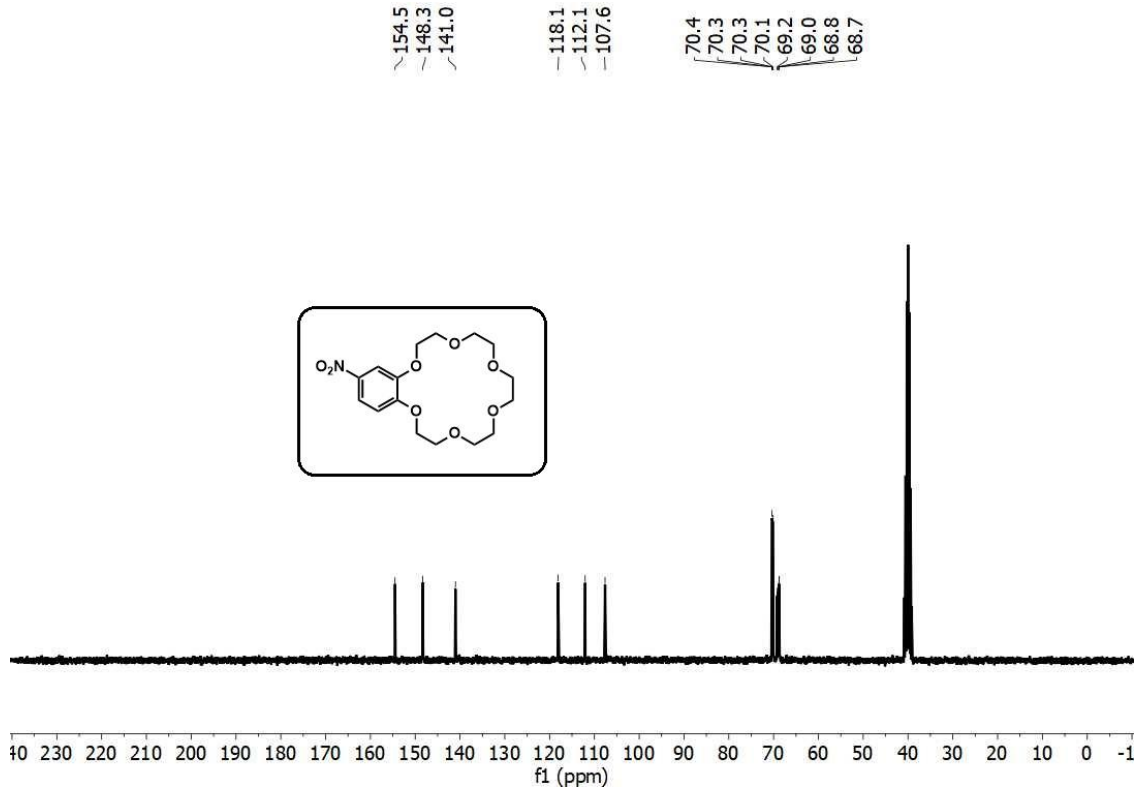
154.5
148.3
141.0
118.1
112.1
107.6
70.4
70.3
70.3
70.1
69.2
69.0
68.8
68.7
f1 (ppm)

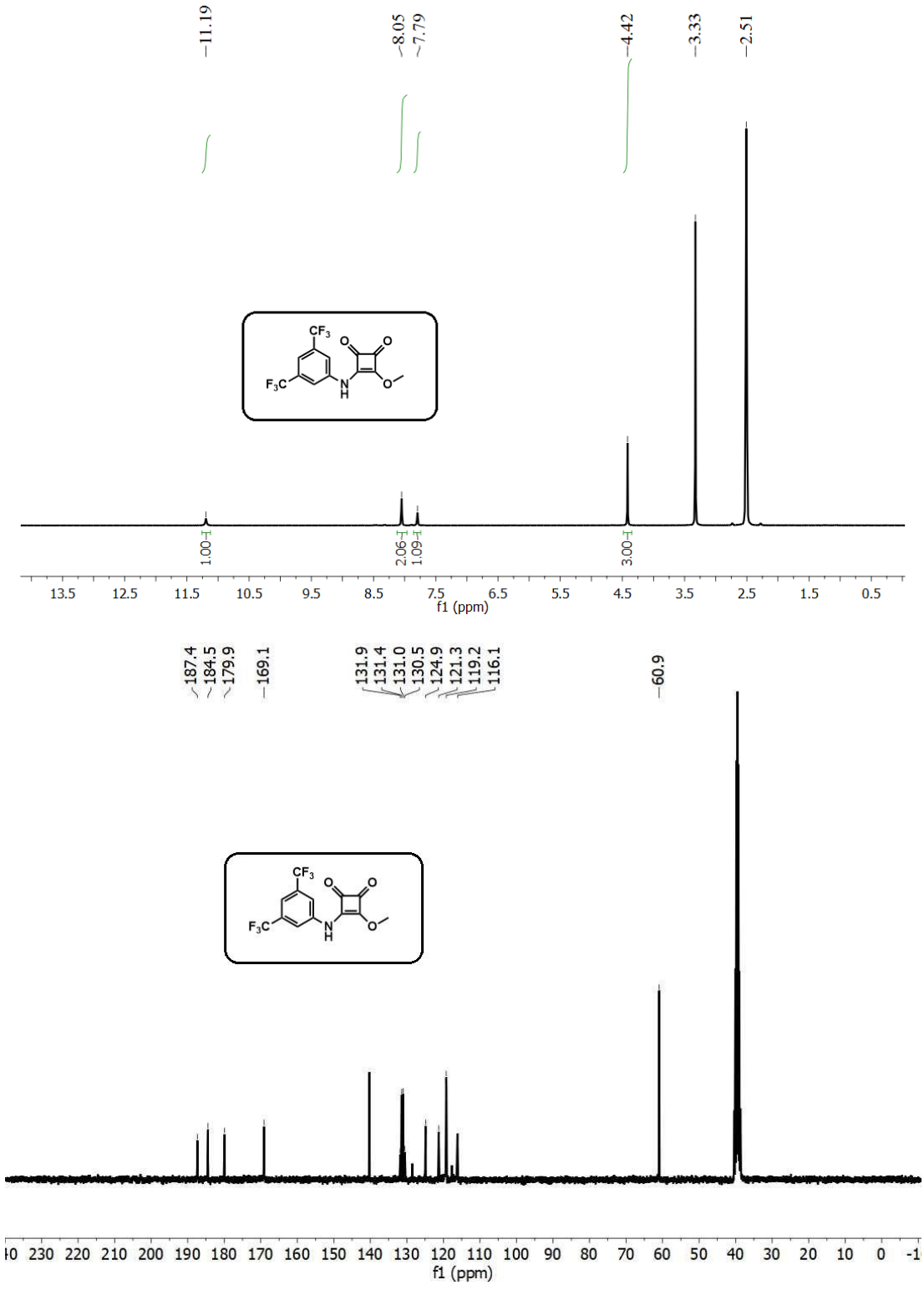
11.19
8.05
7.79
4.42
3.33
2.51
1.00
2.06
1.09
3.00
f1 (ppm)
187.4
184.5
179.9
169.1
131.9
131.4
131.0
130.5
124.9
121.3
119.2
116.1
60.9
f1 (ppm)

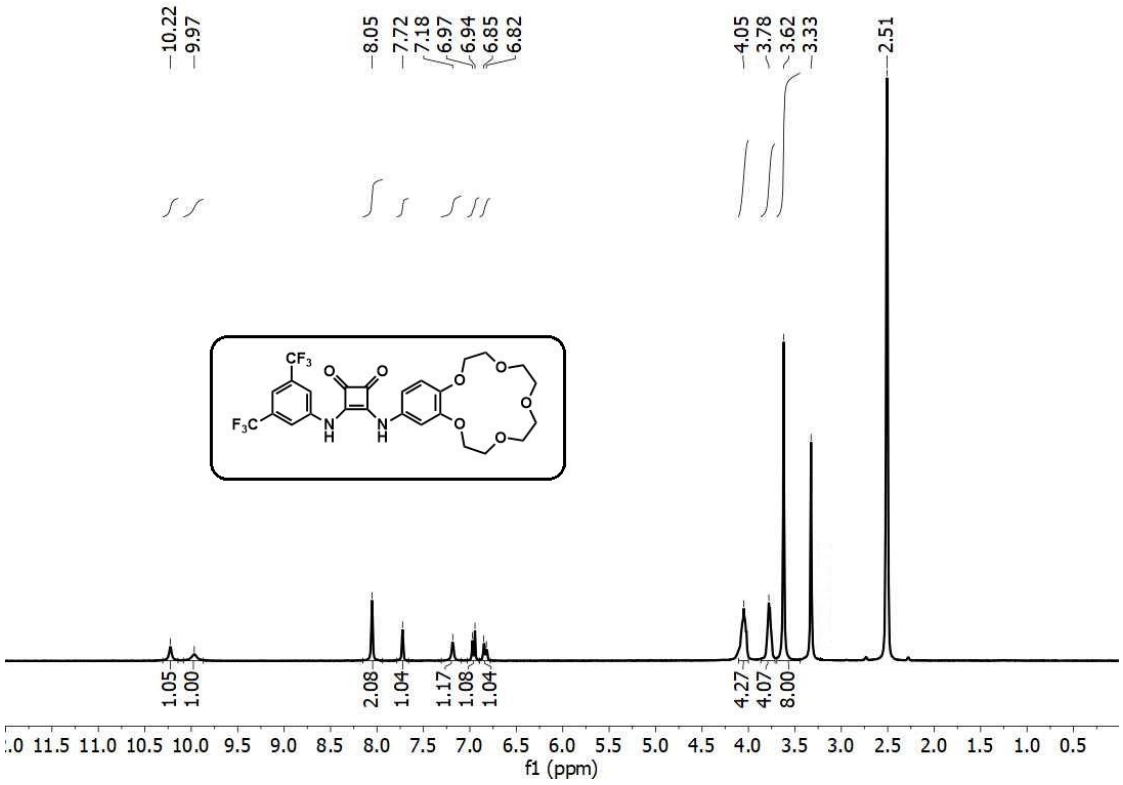
10.22
9.97
8.05
7.72
7.18
6.97
6.94
6.85
6.82
4.05
3.78
3.62
3.33
2.51
1.05
1.00
2.08
1.04
1.17
1.08
1.04
4.27
4.07
8.00
f1 (ppm)

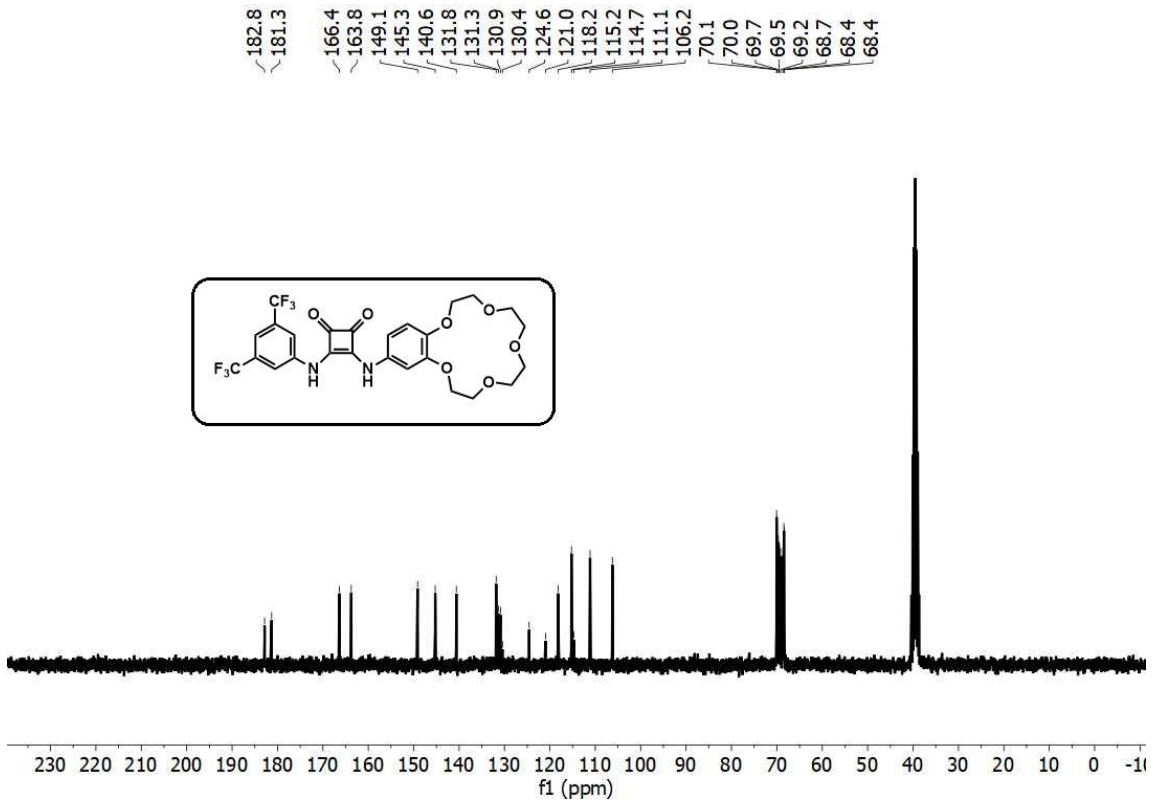
182.8
181.3
166.4
163.8
149.1
145.3
140.6
131.8
131.3
130.9
130.4
124.6
121.0
118.2
115.2
114.7
111.1
106.2
70.1
70.0
69.7
69.5
69.2
68.7
68.4
68.4
f1 (ppm)

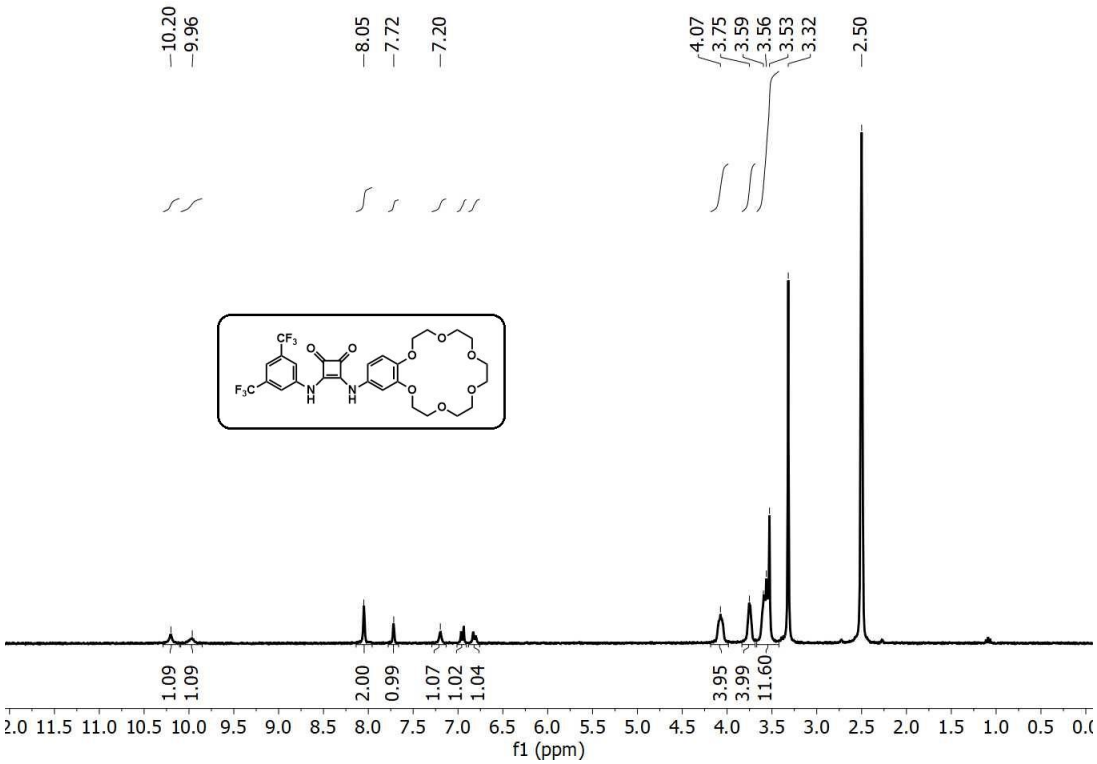
10.20
9.96
8.05
7.72
7.20
4.07
3.75
3.59
3.56
3.53
3.32
2.50
1.09
1.09
2.00
0.99
1.07
1.02
1.04
3.95
3.99
11.60
f1 (ppm)

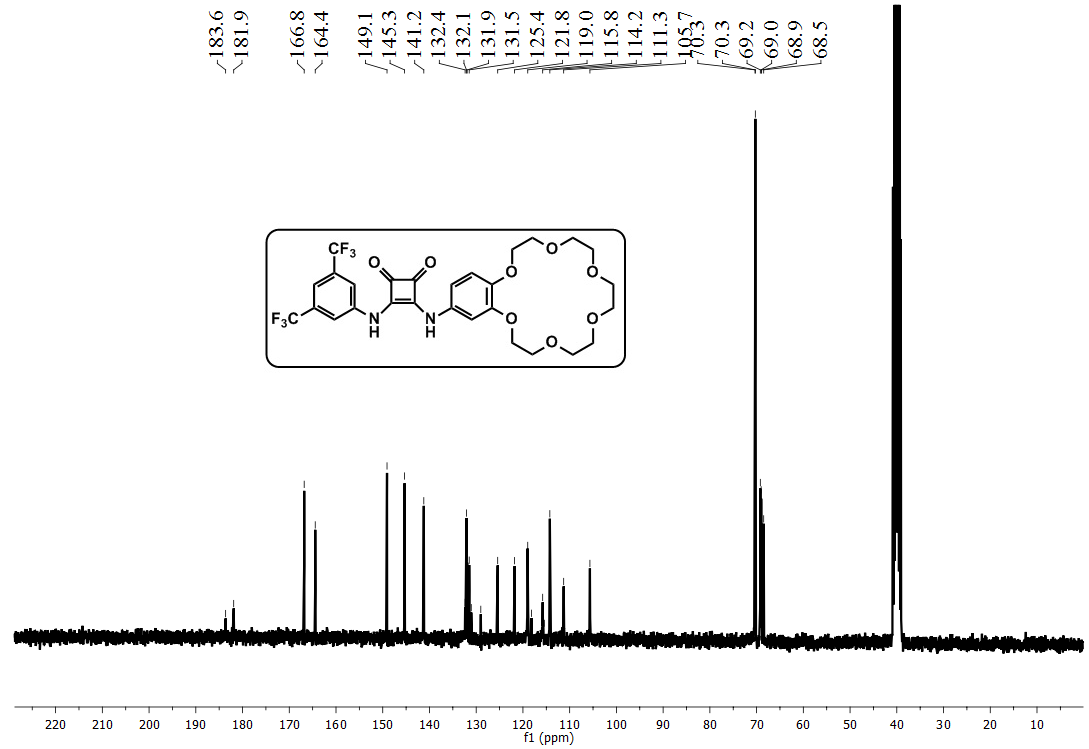
183.6
181.9
166.8
164.4
149.1
145.3
141.2
132.4
132.1
131.9
131.5
125.4
121.8
119.0
115.8
114.2
111.3
105.7
70.3
69.2
69.0
68.9
68.5
f1 (ppm)

LITERATURE

[1] Bruker, *APEX3*, *V2019*, Bruker Nano, Inc., USA.

[2] Bruker, *SAINT*, *V8.41*, Bruker AXS Inc., Madison, Wisconsin, USA.

[3] Bruker, *SADABS, V2016/2 V8.41*, Bruker AXS Inc., Madison, Wisconsin, USA.

[4] L. Krause, R. Herbst-Irmer, G. M. Sheldrick, D. Stalke, *J. Appl. Cryst.* **2015**, *48*, 3–10, doi:10.1107/S1600576714022985.

[5] G. M. Sheldrick, *Acta Cryst.* **2015**, *A71*, 3–8, doi:10.1107/S2053273314026370.

[6] G. M. Sheldrick, *Acta Cryst.* **2015**, *C71*, 3–8, doi:10.1107/S2053229614024218.

[7] C. B. Hübschle, G. M. Sheldrick, B. Dittrich, *J. Appl. Cryst.* **2011**, *44*, 1281–1284, doi:10.1107/S0021889811043202.

[8] D. Kratzert, *FinalCif*, *(Bruker Edition)*, https://dkratzert.de/finalcif.html.

[9] C. F. Macrae, I. Sovago, S. J. Cottrell, P. T. A. Galek, P. McCabe, E. Pidcock, M. Platings, G. P. Shields, J. S. Stevens, M. Towler and P. A. Wood, "Mercury 4.0: from visualization to analysis, design and prediction", *J. Appl. Cryst.*, **2020**, *53*, 226-235, doi:10.1107/S1600576719014092.

[10] R. Evans, G. Dal Poggetto, M. Nilsson, G. A. Morris, "Improving the interpretation of small molecule diffusion coefficients", *Anal. Chem.,* **2018**, *90*, 3987 – 3994.